Flexural and Shear Strengthening of RC Beams with FRP – An Experimental Study

Sarat Chandra Choudhury

Department of Civil Engineering

National Institute of Technology, Rourkela

Odisha, India

November 2012

FLEXURAL AND SHEAR STRENGTHENING OF RC BEAMS WITH FRP –AN EXPERIMENTAL STUDY

A THESIS SUBMITTED IN PARTIAL FULFILLMENT OF
THE REQUIREMENTS FOR THE DEGREE OF

Master of Technology (Research)
in
Structural Engineering

by

Sarat Chandra Choudhury

Roll No. : 609CE312

Under the guidance of

Prof. Shishir Kumar Sahu

Department of Civil Engineering

National Institute of Technology

Rourkela- 769008

November 2012

DEPARTMENT OF CIVIL ENGINEERING

NATIONAL INSTITUTE OF TECHNOLOGY

ROURKELA, ODISHA-769008

CERTIFICATE

*This is to certify that the thesis entitled, "**FLEXURAL AND SHEAR STRENGTHENING OF R.C. BEAMS WITH FRP – AN EXPERIMENTAL STUDY**" submitted by **SARAT CHANDRA CHOUDHURY** bearing roll no. **609CE312** in partial fulfilment of the requirements for the award of **Master of Technology (Research)** degree in C**ivil Engineering** with specialization in **"Structural Engineering"** during 2010-2012 session at the National Institute of Technology, Rourkela is an authentic work carried out by him under my supervision and guidance.*

To the best of my knowledge, the matter embodied in the thesis has not been submitted to any other University / Institute for the award of any Degree or Diploma.

Prof. Shishir Kumar Sahu

Dept of Civil Engineering

National Institute of technology

Rourkela -769008, Odisha

ACKNOWLEDGEMENT

It is with a feeling of great pleasure that I would like to express my most sincere heartfelt gratitude to my supervisor **Prof. Shishir Kumar Sahu**, Professor, Dept. of Civil Engineering, NIT, Rourkela for his encouragement, advice, mentoring and research support throughout my studies. His technical and editorial advice was essential for the completion of this dissertation. His ability to teach, knowledge and ability to achieve perfection will always be my inspiration.

I express my sincere thanks to **Prof. S. K. Sarangi**, Director of NIT, Rourkela, **Prof. N. Roy**, Professor and HOD, Dept. of Civil Engineering, NIT, Rourkela and **Prof. M. Panda**, Professor and Ex- HOD, Dept. of Civil Engineering, NIT, Rourkela for providing me the necessary facilities in the department.

I would also take this opportunity to express my gratitude and sincere thanks to the faculty members of Dept. of Civil Engineering, **Prof. K. C. Patra, Prof. M. R. Barik** and **Prof. K. C. Biswal** for their invaluable advice, encouragement, inspiration and blessings during the project.

I am extremely grateful to **Prof. G. K. Das**, my class mate, who was a source of great inspiration and encouragement during my stay at NIT, Rourkela.

I am indebted to **Mr. Sukumar Behera,** Ex-M.Tech (Structure) student, Dept. of Civil Engineering who was kind enough to spend his valuable time almost daily to teach me computer operations, which was new to me.

I am highly grateful to **Mr. Jyoti Prakash Giri,** M.Tech (Transportation) student, Dept. of Civil Engineering who was kind enough to help me in editing the booklet in the present shape.

I would also express my sincere thanks to **Mr. S. K. Sethi & Mr. R. Lugun,** laboratory staff members of Department of Civil Engineering, NIT, Rourkela and administrative staffs of this department for their timely help.

I would like to thank the almighty for his blessings. I would like to share this happiness with my wife **Uma,** daughters **Archana** and **Arati** who rendered enormous support during the whole tenure of my stay at NIT, Rourkela.

Sarat Chandra Choudhury

Roll No. – 609CE312

About the Author

Sarat Chandra Choudhury passed B.Sc. with distinction from Khallikote college, Brahmapur in 1960 and B.Tech (Hons) in Civil Engineering from Indian Institute of Technology, Kharagpur in 1964. After passing out, joined as Assistant Engineer in Public Works Department (PWD), Govt. of Odisha in 1964, subsequently worked as Executive Engineer and retired as Superintending Engineer in 1998 from Govt. service. During service period, he designed and constructed a large number of Major Buildings, High Level Bridges and Roads. The important building works constructed are MKCG Medical College, indoor hospital and hostel buildings at Brahmapur, extension of High Court building and Jawaharlal Nehru Indoor Stadium at Cuttack and Brahmapur University buildings at Bhanjabihar, Brahmapur. The important bridge works constructed are High Level Bridges over river Badanadi, Rushikulya, Ghodahada, Loharkhandi and Jorou in Ganjam district under World Bank assistance. After retirement, he worked as Senior Project Engineer, Odisha Health Systems Development Project, Govt. of Odisha, faculty member in S.M.I.T, Brahmapur, State Quality Monitor in PWD and Rural Development (RD) Dept., Govt. of Odisha. Presently he is studying M. Tech (Research) in NIT, Rourkela from 2010 to date. Special field of interest are teaching, quality monitoring and impart technical training to field engineers of Govt. of Odisha on construction methodologies of Roads, Buildings and Bridges..

CONTENTS

Abstract

This study deals with experimental investigation for enhancing the flexural and shear capacity of RC beams using Glass fiber reinforced polymers (GFRP) and Carbon fiber reinforced polymers (CFRP). Fifteen concrete beam specimens with dimensions of 110mm width, 200mm height and 1300mm length were fabricated in the laboratory. As per practical consideration of pre-stressed bridge girders, one 30mm diameter longitudinal hole was provided below the neutral axis in the tension zone in all the beams for future strengthening, service lines and other consideration. The geometry of all beams was kept constant, while steel reinforcement varied as per initial design. Out of 15 beams four were control beams. One beam was made without any steel reinforcement strengthened with two layers of GFRP fabrics U- jacketed over the full span. Five beams were weak in flexure, strengthened using GFRP fabrics with varying configurations in higher flexural zone. Four beams were weak in shear, (tied with two 6-Ø stirrups in each support, one 6-Ø stirrup at mid span to keep the grill intact for concreting) strengthened using GFRP fabrics with varying configurations in higher shear zones near both supports. One beam was made weak in shear, strengthened with CFRP fabrics in higher shear zones near both supports. All the beams were simply supported at both ends with 1000mm effective span, 150mm bearings, loaded under more realistic loading conditions, i.e. uniformly distributed loaded (UDL) and tested up to failure by gradually increasing super imposed load. The preparation of concrete surface was done with great care and showed no bond failure in all U-jacketed and inclined stripped beams. One beam bonded with GFRP fabric in the soffit bottom only failed due to debonding.

The flexural and shear capacities of the beams are compared with the theoretical prediction using codal provisions. The experimental deflection of beams are also compared with the theoretical predictions. The beams weak in flexure after strengthening showed remarkable flexural strength with 33% to 83% increase in cracking load capacity with respect to the control beam depending on the configuration of GFRP. The four beams weak in shear after strengthening showed 25% to 81% increase in cracking load capacity with respect to the control beam depending on the configuration of GFRP. One beam shear strengthened with CFRP showed remarkable increase of 131% in cracking load capacity and rigidity with respect to the control beam which is highest in the series of tested beams. There was increase in the stiffness of all strengthened beams compared to the control beams.

List of figures

Figure No.	Title	PageNo.

Figure No.	Title	PageNo.

List of Tables

List of Symbols

f_{ck} Characteristic compressive strength of concrete

f_y Yield strength of steel

V_c Shear capacity of concrete

V_s Shear contribution of steel stirrups and bent up bars

V_{frp} Shear contribution of FRP

V_n Shear strength of a strengthened RC beam

f_{frp} Tensile strength of FRP

Φ_{frp} Reduction factor for the FRP

A_{frp} Cross sectional area of a pair of FRP strips

β Angle of fiber orientation with respect to horizontal direction for the left side of the beam

d Effective depth of beam

s_{frp} Spacing of FRP strips measured along the longitudinal axis

x/z Neutral axis depth

d_{si} Centroid of steel bars in layer 'i' from the extreme concrete compression fiber

d_{frp} Centroid of FRP from the extreme concrete compression fiber

h Depth of the RC beam

ϵ_{cf} Strain at extreme compression fiber of concrete

ϵ_{frp} Strain in the FRP

ϵ_{si} Strain in the steel

ϵ_{co} Compressive strain of unconfined concrete at peak stress

ϵ_u Ultimate compressive strain of concrete

f_{cu} Cube compressive strength of concrete

b Width of beam

K_1 Mean stress factor

σ_{si} Stress in steel bars

σ_{frp} Stress in FRP

A_{si} Total area of steel in layer 'i'

n Total numbers of steel layers

A_{frp} / A_f Area of FRP

K_2 Centroid factor of the compressive force

F_{frp} Tensile strength of FRP

E_{frp} Modulus of elasticity of FRP

γ_{frp} Partial safety factor for FRP tensile strength

γ_s Partial safety factor for steel

γ_c Partial safety factor for concrete in flexure

E_c modulus of elasticity of concrete

E_s modulus of elasticity of steel

E_f modulus of elasticity of FRP

A_{sc} Area of compression steel

A_{st} Area of tension steel

q load per unit length

ℓ effective length of span

d_2 effective cover to compression steel

CHAPTER 1

INTRODUCTION

1.1 Introduction

There are many existing bridge and building structures throughout the world, which do not fulfil specified design requirements. This may be due to upgrading of the design standards, increased loading due to change of use, ageing, corrosion of the reinforcement bars, marginal design, construction errors and poor construction, use of inferior material, and accidents such as fires and earthquakes, which renders the structure incapable of resisting the applied service loads. Thus the structure needs complete replacement or strengthening. The solution in such cases is complete dismantling and new construction or increasing the load carrying capacity through strengthening of the effected structures in various ways. Because of the prohibitive cost of replacing large number of deteriorated structures throughout the world, research efforts have focused on many methods of strengthening of structures. The strengthening and retrofitting of concrete structures represents one of the most challenging problems faced by engineers today.

Historically, steel has been the primary material used to strengthen concrete bridges and buildings. Bonded steel plates or stirrups have been applied externally to successfully strengthen and repair concrete girders that are deficient in flexure or in shear. However, using steel as a strengthening element adds additional dead load to the structure and normally requires corrosion protection. These methods suffer from inherent disadvantages ranging from difficult application procedure to lack of durability. In recent years, the bonding of fiber reinforced polymer (FRP) fabrics, plates or sheets has become a very popular method for strengthening of RC beams. In fact, the application of FRPs to the strengthening of structures was first researched in the middle of 1980s for the flexural strengthening of RC beams using CFRP plates at the Swiss Federal Laboratory for Materials Testing and Research (Meier *et al.* 1993). In recent years, there is extensive research on the use of FRP fabrics, plates or sheets to replace steel plates in plate bonding. FRPs are used widely for beam and column strengthening by external wrapping. At present there are numerous research teams all over the world undertaking research in this area. The main advantages of FRP fabrics, sheets or plates are their high strength-to -weight ratio and high corrosion resistance. The former property leads to great ease in site handling, reducing

labour cost and interruptions to existing services, while latter ensures durable performance. FRP plates are normally at least twice but can be over 10 times as strong as steel plates, while their weight is only 20% of that of steel. FRP composites used in aerospace industry for many years and their superior properties are well known. The limited use of FRP in civil engineering applications is due to their high cost. However, their prices are coming down rapidly, enabling their wider use in civil engineering. For application in the strengthening of structures, the material cost is only one aspect and may be a small portion of the total cost involved including labour cost, loss due to interruptions to services. FRP composites often provide the most cost-effective overall solution to civil engineering applications.

1.2 Methods of Strengthening and Retrofitting

- Use of steel plate and steel jacketing to concrete structures.
- Use of steel bars bonded and unbonded to concrete structures.
- External pre-stressing of bridge girders.
- Chemical treatment.
- Use of FRP composites bonded to concrete using a suitable matrix.

  Flexural and shear strengthening of a simply supported RC beam using FRP composites is generally by bonding of a FRP plate to soffit and webs of the RC beam. The FRP plate may be a prefabricated (pultruded) plate, may be constructed on site in a wet lay-up process.

1.3 Fiber Reinforced Polymer (FRP)

Fiber reinforced composite materials consist of fibers of high strength and modulus embedded in or bonded to a matrix with distinct interfaces between them. In this form, both fibers and matrix retain their physical and chemical identities, yet they produce a combination of properties that cannot be achieved with either of the constituents acting alone. Fibers are the principal load carrying members, while the matrix keeps them in the desired location, orientation and protect them from environmental damages. The fiber imparts the strength, while matrix keeps the fiber in place, transfer stresses between the fibers, provides a barrier against an adverse environment such as chemicals and moisture, protects from abrasion. FRP is an acronym for Fiber Reinforced Polymer and identifies a class of composite materials consisting of brittle, high strength and

stiffness fibers embedded at high volume fractions in ductile low stiffness and strength polymeric resins called matrix.

FRP with polymeric matrix can be considered as a composite. They are widely used in strengthening of civil structures such as beams, girders, slab, columns and frames. There are many advantages of FRP due to light weight, corrosion-resistant, good mechanical properties. The main function of fibers is to carry load, provide strength, stiffness and stability. The function of the matrix is to keep fibers in position and fix it to the structures. There are mainly three types of fibers dominating the civil engineering industry such as glass, carbon and aramid fibers. Each has its own advantages and disadvantages.

1.4 History of FRP

Global polymer production on the scale present today began in the mid-20th century, when low material and production costs, new production technologies and new product categories combined to make polymer production economical. The industry finally matured in the late 1970s when world polymer production surpassed that of Steel, making polymers the ubiquitous material that it is today. Glass fiber reinforcement was tested in military applications at the end of World War II, Carbon fiber production began in the late 1950s and was used, though not widely, in British industry beginning in the early 1960s, aramid fibers were being produced around this time also, appearing first under the trade name Nomex by DuPont. Today each of these fibers is used widely in industry for any applications that require plastics with specific strength or elastic qualities. Indeed, many have hailed FRP, is an excellent composite as a new generation of construction material following steel and concrete.

1.5 Methods of forming FRP composites

FRP composites are formed by embedding continuous fibers in resin matrix, which binds the fibers together. The common resins are epoxy resins, polyester resins and vinylester resins, depending on the fibers used. FRP composites are classified into three types:

- Glass-fiber-reinforced polymer (GFRP) composites
- Carbon-fiber-reinforced polymer (CFRP) composites
- Aramid-fiber-reinforced polymer (AFRP) composites

1.6 Methods of FRP application in structures

The bonding of unstressed FRP plates to the soffit / webs of RC beams is the most common and has received the greatest amount of theoretical and experimental research to date. Three schemes exist for the adhesion of unstressed FRP plate to the soffit / webs of an RC beam. Resin is applied to the concrete surface, and layers of fabric are impregnated in place using steel roller. Here the adhesive also forms the matrix of the FRP and this creates a strong bond with the RC beam. This method is however sensitive to unevenness of the RC beam soffit / webs and such unevenness can lead to debonding of FRP from concrete surface.

1.7 Advantages and disadvantages of FRP

The various advantages of FRP are:

- Corrosion/wear resistance, lowers maintenance and repair costs.
- High specific strength and stiffness
- Fatigue life.
- Thermal and Acoustical insulation.
- Easier application
- Very high tensile strength, but low weight.
- Repair in limited time without effecting traffic flow/service.

  FRP has a great potential for replacing reinforced concrete, and steel reinforcement in bridges, buildings, and other civil infrastructures. Glass fibers are the most common of all reinforcing fibers. Two types of glass fibers commonly used are: (i) E-Glass and (ii) S-Glass.

The disadvantages of FRP are:

- In general compressive strength is lower than the tensile strength.
- Risk of fire and high temperature.
- High cost of carbon fibers.
- Tensile stress-strain diagrams for various reinforcing fibers are almost linear up to the point of failure and have a brittle failure mode.

- Unlike steel reinforcement, it cannot be bent or hooked to provide required anchorage. Poor fire resistance of FRP bars is a serious draw back and hence FRP bars/laminates are not to be proposed for structures where fire is a major design issue.

1.8 Research significance

Numerous old bridges and buildings are in an advanced state of disintegration. The continuing deterioration of the infrastructure highlights the need for effective means of strengthening and rehabilitating of such structures. The strengthening of rectangular RC beams are usually undertaken using fiber reinforced polymer (FRP) fabrics bonded to the beams using epoxy resins. Further, in case of pre-stressed concrete girders in bridges, dummy / service longitudinal cable holes are provided for future strengthening as per need. Similarly, in beams in building dummy longitudinal holes are provided for taking service cables inside and future strengthening as per need. The beams are generally subjected to uniformly distributed loads (UDL) due to self weight and service loads coming over it. Thus, the strengthening of rectangular beams with holes subjected to UDL using FRP is of great technical importance in understanding the flexural and shear behaviour of beams.

A thorough review of earlier works done in this field is an important requirement to arrive at the objective and scope of the present investigation. The detail review of literature along with author's critical discussion is presented in next chapter.

CHAPTER 2

REVIEW OF LITERATURE

2.1 Introduction

A great amount of research is available in the published literature predominately on the strengthening of RC structures using steel rods and plates. However, the increase of dead load triggers searching of alternate lighter material for strengthening of structural elements. Glass fibers are the most common across all industries, although carbon and aramid fiber composites are found in aerospace, automotive and sporting goods applications. Since the late 1990's, there has been rapid growth in the application of FRP composites in construction around the world in terms of both research activities and practical implementations. The FRP is used mostly for either retrofitting or strengthening of RC beams in flexure and shear by external bonding of a plate / sheet to the tension face of a beam.

2.2 Retrofitting of RC beams with external bonding of FRP

The FRP plate bonding technology was first investigated at the Swiss Federal Laboratory for Materials Testing and Research (Meier *et al*. 1993) where tests on RC beams strengthened with CFRP plates started in 1984. The research projects were undertaken in around 1993 in USA and Canada in the areas of CFRP to use this material in construction. The main advantages of FRP plates are their high strength- to- weight ratio and corrosion resistance. The former property leads to great ease in site handling, reducing labour cost and interruption to exiting services, while the latter ensures durable performance. FRP plates are normally twice but can be over 10 times as strong as steel plates while their weight is only 20% of that of steel (Meier *et al*. 1993, Darby 1999).Buyukozturk and Hearing (1998) investigated the rehabilitation and retrofit of damaged reinforced concrete beams. Flexural strength was enhanced with this method but the failure behaviour became more brittle, often involving delamination of the composite and shear failure of the beams. Physical models of reinforced concrete beams with variations in shear strengths, bonded laminate lengths, and epoxy types were precracked, then retrofitted with glass and carbon fiber-reinforced plastics and tested in an experimental programme.

Sheikh (2002) studied on retrofitting with fiber reinforced polymers (FRP) to strengthen and repair damaged structures, which was a relatively new technique. At the University of Toronto, application of FRP in concrete structures was investigated for its effectiveness in enhancing structural performance both in terms of strength and ductility. The structural components tested included slabs, beams, columns and bridge culverts. Research on columns had particularly focused on improving their seismic resistance by confining them with FRP. Einde *et al.* (2003) examined that fiber reinforced polymer (FRP) composites or advanced composite materials are very attractive for use in civil engineering applications due to their high strength-to-weight and stiffness-to-weight ratios, corrosion resistance, light weight and potentially high durability. Their application was of most important in the renewal of constructed facilities infrastructure such as buildings, bridges, pipelines, etc. Hadi (2003) examined the strength and load carrying capacity enhancement of reinforced concrete beams, those had been tested and failed in shear. A total of sixteen sheared beam specimens were retrofitted by using various types of fiber reinforced polymer (FRP) and then retested. The retrofitted beam specimens wrapped with different amounts and types of FRP were subjected to four-point static loading. Load, deflection and strain data were collected during testing the beam specimens to failure.

Lee and Hausmann (2003) studied the load capacity, ductility and energy absorption aspects of reinforced concrete (RC) beams retrofitted with sprayed fiber-reinforced polymer composites (SFRP). It was also intended to assess the feasibility of using SFRP for repair and strengthening of damaged RC beams. A series of three-point bending tests were conducted on both damaged (pre-cracked) and undamaged RC beams to evaluate the performance of deteriorated RC beams after application of SFRP and to examine the influence of SFRP parameters on the performance of RC beams. The parameters in the experimental programme were coating thickness, fiber length, fiber materials and fiber loading.

Rabinovitch and Frostig (2003) studied strengthening, upgrading, and rehabilitation of existing reinforced concrete structures using externally bonded composite materials. Five strengthened, retrofitted, or rehabilitated reinforced concrete beams were experimentally and analytically investigated. Emphasis was placed on the stress concentration that arises near the edge of the fiber reinforced plastic strip, the failure modes triggered by these edge effects, and the means for the prevention of such modes of failure. Three beams were tested with various edge

configurations that include wrapping the edge region with vertical composite straps and special forms of the adhesive layer at its edge. The last two beams are preloaded up to failure before strengthening and the ability to rehabilitate members that endured progressive or even total damage was examined. Wu and Davies (2003) developed a theoretical method to predict the loading capacity of a cracked FRP reinforced concrete flexural beam. The beam subjected to three-point bending was externally reinforced with unidirectional FRP plate near the bottom surface of the tensile zone. No slip between the FRP plate and plain concrete was assumed. A fictitious crack approach which had been used previously in conjunction with finite element method in the fracture analysis of concrete was adopted to estimate the equivalent bridge effect of the fracture process zone of concrete. Anania *et al.* (2005) investigated on the use of FRP composites as the most promising technologies for repairing, strengthening or retrofitting of existing structures to resist higher loads and to rectify damage.

Li and Ghebreyesus (2006) experimented with prepared beams, precracked by four-point bending to simulate heavily damaged RC beams. The damaged beams were then surface prepared using sand-blasting and repaired using E-glass fiber-reinforced ultraviolet (UV) curing vinyl ester. The repairs were fully cured by exposure to an UV-A light source for one hour. The repaired beams were again subjected to four-point bending test, this time until failure. The effectiveness of UV curing FRP on fast repairing damaged RC beams was evaluated based on the test results.

Wang *et al.* (2007) investigated the practical application of composite materials for retrofitting of reinforced concrete bridge T-sectional girders. Carbon and glass fiber-reinforced polymers (CFRP and GFRP) saturated in an epoxy resin matrix were used to enhance the service load-carrying capacity of the bridge. Three 5m long simply supported beams were tested under monotonic and cyclic loads for comparison to a beam subjected to more than 10^6 cycles in the service load range. Yang *et al.* (2007) studied retrofitting of reinforced concrete (RC) beams bonded with fiber-reinforced polymer (FRP) plates to their soffits. An important failure mode of such plated beams was debonding of the FRP plates from the concrete due to high level interfacial stresses near the plate ends. A closed-form rigorous solution for the interfacial stresses in simply supported beams bonded with thin plates and subjected to arbitrary loads had been found, in which a non-uniform stress distribution in the adhesive layer was taken into account.

Al-Saidy *et al.* (2010) studied experimentally results of damaged/repaired RC beams strengthened with CFRP. The experimental programme consisted of RC rectangular beam specimens exposed to accelerated corrosion. The corrosion rate was varied between 5% to 15% which represents loss in cross-sectional area of the steel reinforcement in the tension side. Corroded beams were repaired by bonding CFRP sheets to the tension side to restore the strength loss due to corrosion. Different strengthening schemes were used to repair the damaged beams.
Martinola *et al.* (2010) examined the use of a jacket made of fiber reinforced concrete with tensile hardening behaviour for strengthening of R C beams by means of full-scale tests on 4.55 m long beams. A 40 mm jacket of this material was directly applied to the beam surface. Both the strengthening and the repair of RC beams were studied. In particular, in the latter case the beam was initially damaged and eventually repaired. A numerical analysis was also performed in order to better understand the reinforcement behaviour.
Kim and Shin (2011) studied RC beams retrofitted with new hybrid FRP system consisting carbon FRP (CFRP) and glass FRP (GFRP). The objective of study was to examine effect of hybrid FRPs on structural behaviour of retrofitted RC beams and to investigate if different sequences of CFRP and GFRP sheets of the hybrid FRPs have influences on improvement of strengthening RC beams. RC beams were fabricated and retrofitted with hybrid FRPs having different combinations of CFRP and GFRP sheets. The beams were loaded with different magnitudes prior to retrofitting in order to investigate the effect of initial loading on the flexural behaviour of the retrofitted beams. The main test variables were sequences of attaching hybrid FRP layers and magnitudes of preloads. Under loaded condition, beams were retrofitted with two or three layers of hybrid FRPs, loads increased until the beams reached failure.
Obaidat *et al.* (2011) studied the results of an experimental study to investigate the behaviour of structurally damaged full-scale reinforced concrete beams retrofitted with CFRP laminates in shear or in flexure. The main variables considered were the internal reinforcement ratio, position of retrofitting and the length of CFRP. The experimental results, generally indicate that beams retrofitted in shear and flexure by using CFRP laminates are structurally efficient and are restored to stiffness and strength nearly equal to or greater than those of the control beams.

2.3 Flexural Capacity of RC beams with external bonding of FRP

Chajes *et al.* (1994) investigated on the ability of externally bonded composite fabrics to improve the beams flexural capacity by testing a series of reinforced concrete beams with two point loading to determine the ability of externally bonded composite fabrics to improve the beams' flexural capacity. The fabrics used were made of aramid, E-glass and graphite fibers, and were bonded to the beams using a two-part epoxy. The different fabrics were chosen to allow a variety of fabric stiffnesses and strengths to be studied. The external composite fabric reinforcement led to increase in flexural capacity and stiffness. For the beams reinforced with E-glass and graphite fiber fabrics, failures were a result of fabric tensile failure in the maximum moment region. Shahawy *et al.* (1995) studied flexural behaviour of reinforced concrete rectangular beams with epoxy bonded carbon fiber reinforced plastic (CFRP) laminates. The test type of load data were presented on the effect of CFRP laminates, bonded to the soffit of a beam, on the first crack load, cracking behaviour, deflections, serviceability loads, ultimate strength and failure modes. The increase in strength and stiffness provided by the bonded laminates was assessed by varying the number of laminates. Duthinh and Starnes (2001) tested seven concrete beams reinforced internally with steel and externally with carbon FRP laminate applied after the concrete had crackcd under two point loading**.**

Smith and Teng (2001) investigated bonding of a fiber reinforced polymer (FRP) plate to the tension face of a beam which has become a popular flexural strengthening method in recent years. As a result, a large number of studies have been carried out in the last decade on the behaviour of these FRP-strengthened beams. Many of these studies reported premature failures by de-bonding of the FRP plate with or without the concrete cover attached. The most commonly reported de-bonding failure occurs at or near the plate end, by either separation of the concrete cover or interfacial de-bonding of the FRP plate from the RC beam. In this paper, a comprehensive review of existing plate de-bonding strength models was presented. Leung *et al.* (2002) investigated the bonding of fiber reinforced plastic (FRP) plates as an effective and efficient method to improve the bending capacity of concrete beams. In the literature, various design methodologies were proposed and several of them have been found to compare well with test data or to provide reasonable lower bounds. However, almost all the experimental data were obtained from laboratory-size specimens that are several times smaller than the actual beams. In

this investigation, geometrically similar reinforced concrete beams with steel ratio of 0.01, and depth ranging from 0.2 m to 0.8 m were prepared. Some RC beams were tested as control while others were retrofitted with 2 to 8 layers of Carbon fiber reinforced plastic (CFRP) sheets to achieve the same CFRP/concrete area ratio.

Pham and Al-Mahaidi (2004) examined reinforced concrete beams retrofitted with fiber reinforced polymer composites (FRP) to enhance its flexural capacity can experience several failure modes, namely flexural, end debond and midspan debond failures . The mechanism of these failures and available prediction models were first identified in the paper. The models were then assessed with an up to date database of beams reported in literature together with beams tested by the authors. Pesic and Pilakoutas (2005) studied the flexural analysis of RC beams with externally bonded FRP reinforcement. A numerical method was developed for the computation of bending moment capacity of FRP plated RC beams and prediction of the flexural failure modes. The expressions for the upper and lower values of the characteristic plate reinforcement ratios were derived for rectangular and T-sections using the Euro code 2 models for concrete.
Esfahani *et al.* (2007) investigated the flexural behaviour of reinforced concrete beam strengthened using Carbon Fiber Reinforced Polymers (CFRP) sheets. The effect of reinforcing bar ratio on the flexural strength of the strengthened beams was examined. Twelve concrete beam specimens were manufactured and tested. Beam sections with three different reinforcing ratios were used as longitudinal tensile reinforcement in specimens. Nine specimens were strengthened in flexure by CFRP sheets. The other three specimens were considered as control specimens. Gorji (2009) presented a model for calculation of deflection of reinforced concrete **(**RC) beams and columns strengthened in flexure through the use of FRP composites using the potential energy. The validity of the proposed model was verified by comparing with the results of the finite element model.

2.4 Shear Capacity of RC beams with external bonding of FRP

Khalifa and Nanni (2000) presented the shear performance of reinforced concrete (RC) beams with T-section. Different configurations of externally-bonded carbon fiber-reinforced polymer (CFRP) sheets were used to strengthen the specimens in shear. The experimental programme consisted of six full-scale simply supported beams. One beam was used as a bench mark and five beams were strengthened using different configurations of CFRP. The parameters investigated in

the study included wrapping schemes, CFRP amount, 90°/0° ply combination, and CFRP end anchorage. Chen and Teng (2003) studied on shear strengthening of reinforced concrete beams by externally bonding fiber reinforced polymer (FRP) composites. Those studies have established clearly that such strengthened beams fail in shear mainly in one of two modes: FRP rupture and FRP debonding, and have led to preliminary design proposals. The study was concerned with the development of a simple, accurate and rational design proposal for the shear capacity of FRP-strengthened beams which fail by FRP debonding. Existing strength proposals were reviewed and their deficiencies highlighted. A new strength model was then developed. The model was validated against experimental data collected from the existing literature.

Al-Amery and Al-Mahaidi (2006) experimentally investigated the coupling of shear-flexural strengthening of R C beams. The presence of shear straps to enhance shear strength has the dual benefit of delaying de-bonding of CFRP sheets used for flexural strengthening. Six RC beams were tested having various combinations of CFRP sheets and straps in addition to a strengthened beam as control test. The instrumentation used in these tests cover the strain measurements in different CFRP layers and located along the span, in addition to the slip occurring between the concrete and CFRP sheets.

Bencardino *et al.* (2007) investigated the effectiveness of externally bonded reinforcement of a strengthened Reinforced Concrete (RC) beam subjected to a shear dominant loading regime. The aim of this paper was to clarify the structural performance of RC beams without any internal shear reinforcement but Strengthened with Carbon Fiber Reinforced Polymer (CFRP) laminates when the primary mode of failure of the unstrengthened beam was in shear. Four RC beams were specifically designed without and with an externally anchorage system, which was carefully detailed to enhance the benefits of the strengthening lamina and counteract the destructive effects of shear forces. The beams mentioned were tested under two point loading and extensively instrumented to monitor strains, cracking, load capacity and failure modes. Sas *et al. (*2008) reported that the shear failure of reinforced concrete beams needs more attention than the bending failure since no or only small warning precedes the failure. For this reason, it is of utmost importance to understand the shear bearing capacity and also to be able to undertake significant rehabilitation work if necessary. In this paper, a design model for the shear strengthening of concrete beams by using fiber reinforced polymers (FRP) was presented, and the limitations of the truss model analogy were highlighted.

Sundarraja and Rajamohan (2009) studied on shear strengthening of RC beams using externally bonded fiber reinforced polymer sheets. The objective was to clarify the role of glass fiber reinforced polymer inclined strips epoxy bonded to the beam web for shear strengthening of reinforced concrete beams. Included in the study were effectiveness in terms of width and spacing of inclined GFRP strips, spacing of internal steel stirrups, and longitudinal steel rebar section on shear capacity of the RC beam. The study also aimed to understand the shear contribution of concrete, shear strength due to steel bars and steel stirrups and the additional shear capacity due to glass fiber reinforced polymer strips in a RC beam, to study the failure modes, shear strengthening effect on ultimate force and load deflection behavior of RC beams bonded externally with GFRP inclined strips on the shear region of the beam. El-Maaddawy and El-Ariss (2012) presented test results of 16 reinforced concrete beams with web openings strengthened in shear with externally bonded carbon fiber reinforced polymer (CFRP) composite sheets. No internal web reinforcement was provided in the test region to resemble the case of inclusion or enlargement of an opening in an existing beam which would typically result in cutting the internal web reinforcement around the opening. The test parameters were the width and depth of the opening and the amount of the CFRP sheets used for shear strengthening.

2.5 Debonding mode of failure of RC beams with external bonding of FRP

Varastehpour and Hamelin (1997) examined by strengthening of a reinforced concrete beam in situ by externally-bonded fiber reinforced polymer (FRP). For the experimental determination of the mechanical properties of the concrete/glue/plate interface, a new test was suggested. An iterative analytical model capable of simulating the bond slip and the material non-linearity, based on the compatibility of deformations and the equilibrium of forces was developed in order to predict the ultimate forces and deflections. Finally, a series of large-scale beams strengthened with fiber reinforced plastic was tested up to failure. Load deflection curves were measured and compared with the predicted values to study the efficiency of the externally bonded plate and to verify the test results. Mohamed Ali *et al.* (2001) studied the design rules already developed for adhesive bonding of steel plates to reinforced concrete beams in order to prevent premature debonding by either shear peeling or flexural peeling and to determine experimentally whether those design rules that were developed for steel plated beams and slabs, could be applied to fiber reinforced plastic (FRP) plated beams.

Smith and Teng (2002) studied RC beams strengthened in flexure by the bonding of a FRP plate to the tension face susceptible to brittle debonding failures. Such failures commonly initiate at or near one of the plate ends at a load below that to achieve flexural failure of the plated section. For a successful design of flexural strengthening using FRP composites, it was important to be able to predict such plate end debonding failures. The aim of the paper was to provide a comprehensive assessment of the strengths and weaknesses of all the 12 models. debonding was presented. Perera *et al.* (2004) studied the effect of bonding between concrete and composite plates, when epoxy adhesive was used, which was the objective of this paper. The results of an analytical and experimental study on the behaviour of concrete blocks joined with carbon–fiber-reinforced polymer (CFRP) plates were discussed in this paper. For it, several specimens were tested through adherence tests. Numerical analysis included nonlinear finite element modelling incorporating a damage material model for concrete

Pham and Al-Mahaidi (2004) studied end cover separation and shear crack debond were the two most critical de-bonding modes in beams retrofitted with FRP due to the brittle nature of the failures. A testing programme including 18 rectangular reinforced concrete beams was carried out to investigate the failure mechanisms and the influence of several parameters on these debond modes. Yao *et al.* (2005) studied the behaviour of bond between FRP and concrete which was a key factor controlling the behaviour of concrete structures strengthened with FRP composites. The article presented an experimental study on the bond shear strength between FRP and concrete using a near-end supported (NES) single-shear pull test.

Oehlers (2006) analyzed the design of reinforced concrete (RC) flexural members such as beams, slabs and columns which was intrinsically based on the inherent ductility of the member. In reinforced concrete beams and slabs, ductility is generally achieved by using under-reinforced sections and generally governed by the neutral axis depth parameter K_u which requires ultimate failure by concrete crushing at a specified strain ϵ_c. As the plates of fiber reinforced polymer (FRP) plated RC beams can fracture or debond before the concrete crushes at strain ϵ_c, the ku approach is not directly applicable.

Chen *et al.* (2007) studied that concrete beams could be strengthened by bonding a FRP plate to the tension face. A common failure mode for such beams involves the debonding of the FRP plate that initiates at a major flexural crack, which was widely referred to as intermediate

crack (IC) debonding. To understand IC and other debonding failures, the bond behaviour between FRP and concrete had been studied extensively using simple pull-off tests, in which a plate was bonded to a concrete prism and was subjected to tension. The behaviour of the FRP-to-concrete interface in a beam could be significantly different from that captured in a pull-off test. In a beam, whether debonding along the FRP-to-concrete interface occurs at a major flexural crack or not depends on the conditions at this crack as well as at the adjacent crack on the path of the debonding propagation. Gao *et al.* (2007) studied various methods developed for strengthening and rehabilitation of RC beams. External bonding of fiber reinforced plastic (FRP) strips to the beam has been widely accepted as an effective and convenient method.

Reza Aram *et al.* (2008) studied different types of de-bonding failure modes of beams. Then, experimental results of four-point bending tests on FRP Strengthened RC beams are presented and de-bonding failure mechanisms of strengthened beams are investigated using analytical and finite element solutions. Wang and Hsu (2008) studied the practical applications for the use of fiber reinforced polymer (FRP) composite materials for the seismic strengthening of reinforced concrete beams that have been constructed with a substandard beam bar termination method. Results suggest that the cut-off reinforced concrete beam design does not meet the standard design codes and that if no extra shear reinforcement is arranged in the curtailed region, the beam may be subject to brittle failure. Installation of FRP plates for flexural and shear strengthening can successfully correct the deficiency.

Wang and Hsu (2009) analysed a design approach for strengthening reinforced concrete beams with externally bonded FRP laminates. The use of staggered FRP laminate bonding to the tension face of the beam was suggested as an economical design. The FRP development length suggested in the guidelines was adopted. It was recommended that the FRP U-shaped strips be mechanically anchored so as to increase the longitudinal FRP bond strength and enhance the beam's shear strength. Ceroni (2010) experimentally studied on RC beams externally strengthened with carbon Fiber Reinforced Plastic (FRP) laminates and Near Surface Mounted (NSM) bars under monotonic and cyclic loads. The latter ones characterized by a low number of cycles in the elastic and post-elastic range. Realfonzo and Napoli (2011) presented a large database including results from compression tests performed on over 450 concrete cylinders externally wrapped with Fiber Reinforced Polymer materials. Alfano *et al.(*2012) experimentally investigated on the midspan debonding failure of RC beams retrofitted in flexure

by means of the application of a FRP lamina externally applied to concrete substratum. Experimental tests on a series of RC beams with different geometries and type of internal steel reinforcing bars had been carried out in four-point bending up to failure to evaluate the influence of flexural/shear cracks on the debonding of FRP reinforcement from concrete substratum.

2.6 Critical discussion

Most existing research on FRP plate bonding for rehabilitation and retrofit of damaged structural systems were carried out during last one and half decades (e.g. Buyukozturk and Hearing 1998, Sheikh 2002, Einde *et al*. 2003, Hadi 2003, Lee and Hausmann 2003, Rabinovitch and Frostig 2003, Wu and Davies 2003, Anania *et al*. 2005, Li and Ghebreyesus 2006, Wang *et al*. 2007, Yang *et al.* 2007, Al-Saidy *et al*. 2010, Martinola *et al.* 2010, Kim and Shin 2011, Obaidat *et al.* 2011). The structural components tested so far were beams and girders in bridge culverts. The specimens tested were in small scale to full scale models of the structural components generally used in the field. Results so far indicate that retrofitting with FRP offers an attractive alternate to the traditional techniques such as using steel rods, plates or jackets to enhance the strength of the member successfully, but the specimens were observed to fail through a variety of mechanisms. The loading applied was confined to one or two concentrated loads on the span.

Few research work on FRP plate bonding for flexural strengthening had been carried out in the last one and half decades (e.g. Chajes et al. 1994, Shahawy et al. 1995, Duthinh and Starnes 2001, Smith and Teng 2001, Leung et al. 2002, Pham and Al-Mahaidi 2004, Pesic and Pilakoutas 2005, Esfahani et al. 2007) to enhance flexural capacity of beams and bridge girders. The specimens tested were either small scale or full scale models of the structural components generally adopted in the field. Gorji (2009) predicted the deflection of simply supported uniformly distributed loaded RC beams strengthened by FRP composites applying energy variation method and compared with finite element model.

Research studies on the shear strengthening of RC beams was carried out since early 2000s (e.g. Khalifa and Nanni 2000, Chen and Teng 2003, Al-Amery and Al-Mahaidi 2006, Bencardino *et al.* 2007, Sas *et al.* 2008, Sundarraja and Rajamohan 2009, El-maaddawy and El-Ariss 2012), but the work is much more limited compared with that on rehabilitation and retrofitted beams. The loading system was either one or two concentrated loads on the tested beams. So, more research is needed to utilize the full potential of FRP shear strengthening of beams.

Substantial experimental and theoretical work exists on the bond strength, debonding failure modes of FRP bonded to the concrete surface. Experiments had been carried out using several set-ups (e.g. Varastehpour and Hamelin 1997, Mohamed Ali *et al.* 2001, Smith and Teng 2002, Perera *et al.* 2004, Pham and Al-Mahaidi 2004, Yao *et al.* 2005, Oehlers 2006, Chen *et al*. 2007, Gao *et al.* 2007, Reza Aram *et al.* 2008, Wang and Hsu 2008, 2009, Ceroni 2010, Realfonzo and Napoli 2011, Alfano *et al.* 2012) to study the shear and flexural debonding mechanisms, strength development between FRP and RC beams.

From the review of literature, it was observed that some testing of FRP strengthened rectangular beams was carried out over the last two decades. A number of failure modes were observed in RC beams bonded with FRP in flexural and shear zones in all experimental studies. All these studies were confined to one or two points loading only. But, rare attention was paid to the structural behaviour of RC beams subjected under more realistic loading conditions such as uniformly distributed loads (UDL) and with longitudinal service holes met in almost all field conditions strengthened with FRP. Thus this experiment was done for rectangular beams subjected to number of concentrated loads equivalent to UDL and with one longitudinal service hole, strengthened in dominant flexural and shear zones with different types, configuration and layers of FRP which was rare in the previous studies.

2.7 Objective and Scope of Present Research

The objective of present research is to study the performance and behaviour of glass and carbon fiber reinforced polymer strips bonded in single and multilayers in maximum flexural and shear zones of a simply supported rectangular RC beam having a 30 mm diameter longitudinal service hole along the beam below the neutral axis in the tension zone subjected to more realistic loading conditions such as uniformly distributed load (UDL) faced in the field. The hole is provided for future strengthening, prestressing and taking service lines as may require during the service period of the structure. The geometry of all the beams is kept constant throughout the experiment. But the tensile and shear reinforcement of the beams was varied to make few beams weak in flexure and weak in shear respectively. The extent of increase in flexural and shear strength due to GFRP/CFRP U- jacketing in one layer and multilayers, the failure modes such as deflection at quarter span, mid span, initial cracking and ultimate load carrying capacity are studied due to GFRP/CFRP strengthening of the beams.

The different modules of experimental investigations are :

- Study of shear / flexural behaviour of concrete beams subjected to uniformly distributed load.
- Flexural strengthening of beams subjected to uniformly distributed load.
- Shear strengthening of beams subjected to uniformly distributed load.
- The effects of GFRP/CFRP strengthening on initial, ultimate load carrying capacity, deflection and failure pattern of beams subjected to uniformly distributed load.

CHAPTER 3

THEORY AND FORMULATION

3.1 Introduction

This chapter presents the mathematical formulation for flexural and shear strength of control and FRP strengthened RC rectangular beam. The beam is having a longitudinal service hole and subjected to multiple concentrated loads to idealise this as a beam subjected to uniformly distributed load as per practical consideration. The behaviour of the beam subjected to multiple concentrated loads is assumed to be similar to that of under uniformly distributed load.

3.2 Analytical study

Analytical study is made for 15 concrete beams of same geometry, but reinforcement varying in each beam. The control beams are analyzed using limit state method (LSM) and ultimate load method (ULM) of analysis. Five beams are made weak in flexure, strengthened in flexure with bonded GRFP strips are analyzed using British code BS 8110-1997. Five beams are made weak in shear, strengthened in shear with bonded GFRP and CFRP strips are analyzed using the ACI format ACI 318-95-1999. One beam made without any steel reinforcement is also strengthened with bonded GFPR fabric for the full span length, analyzed using British code. The moment of resistance and initial cracking load is calculated for each beam as detailed below.

3.3 Moment of Resistance of RC beams

The moment of resistance of all RC beams are calculated using limit state method of design as per IS 456 - 2000.

3.3.1 Limit State Method of design (IS 456 - 2000)

Considering partial factor of safety = 1

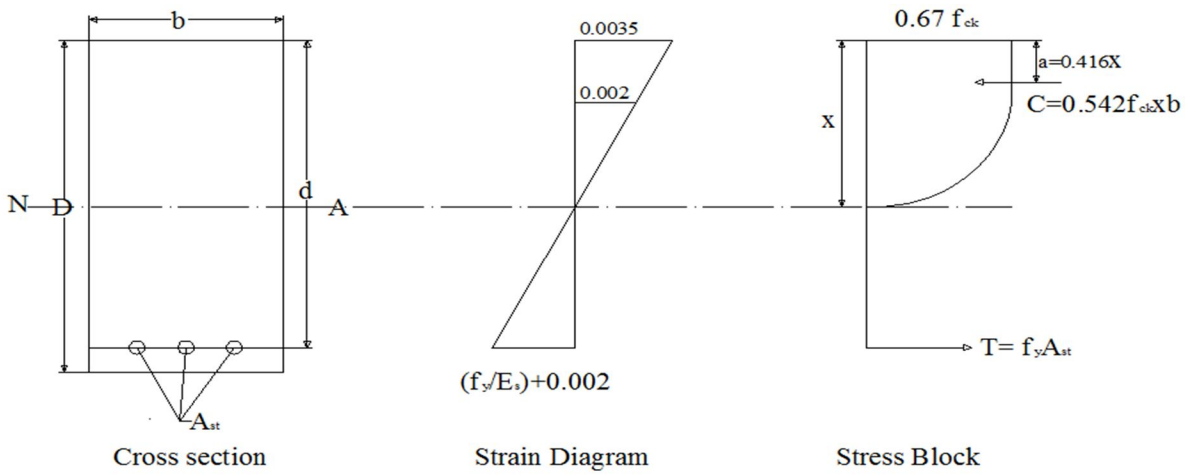

Fig. 3.1 Stress block parameters for LSM

Assume stress in concrete in top most compression fiber $=0.67f_{ck}$

Maximum compressive stress in concrete without partial safety factor $=k_1f_{ck} = 0.67f_{ck}$

Force of compression, $C=0.542f_{ck}$ x b

Let 'a' be the CG distance of force of compression from the extreme top fiber,

a= 0.416x

Lever arm, Z = d-a

$$Z= d - \frac{0.7675}{fck\ b} \times f_y A_{st}$$

Moment of resistance (MR) with respect to concrete = $0.542f_{ck}$ x b Z

Moment of resistance (MR) with respect to steel = $f_y A_{st} Z$

Maximum depth of neutral axis,

$$\frac{x_m}{d} = \frac{0.0035}{0.0055 + \frac{fy}{Es}}$$

As per IS 456-2000, assume $E_s = 2\times10^5$ N/mm^2, Average f_y as per experiment = 531 N/mm^2

$x_m = 0.429\ d$

$M_{lim} = 0.542 f_{ck}\ x\ b\ (d-a)$

$M_{lim} = 0.191 f_{ck}\ b\ d^2$ with respect to concrete

MR with respect to steel = $f_y\ A_{st}\ (d-a)$

$M_{lim} = 0.822 f_y\ A_{st}\ d$ with respect to steel

3.3.2 Ultimate Load Method of design (Whitney's Theory**)**

There are many theories in practice, out of which Whitney's theory (37) has been the most popular and applied to calculate moment of resistance and initial cracking load.

Whitney's Theory

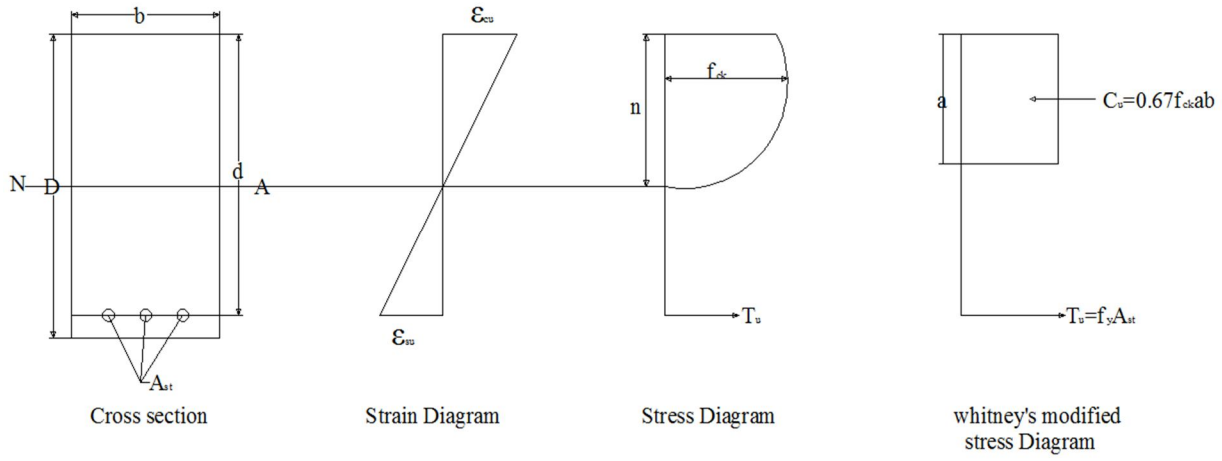

Fig. 3.2 Stress block parameters for ULM

I. Area of the actual curved stress block at ultimate condition= area of rectangular stress block.

II. The line of action of resultant compressive force is the same for two stress blocks given above.

III. The depth of stress block, a = 0.85×actual depth of neutral axis, i.e a = 0.85n Where, n is the actual neutral axis.

IV. The uniform stress of the rectangular stress block = $\frac{2}{3} f_{ck}$

At ultimate stage,

Total compressive force, C_u = Total tensile force T_u

$b \times a \times \frac{2}{3} f_{ck} = A_{st} f_y$

$a = \frac{Ast\ fy}{2/3 fck\ b}$ = the depth of rectangular stress block

Ultimate Moment of resistance

$M_u = C_u \times$ lever arm $= b \times a \times \frac{2}{3} f_{ck} (d - \frac{a}{2})$ with respect to concrete

$M_u = T_u \times$ lever arm $= A_{st} f_y (d - \frac{a}{2})$ with respect to steel

For balanced section, the depth of stress block, a= 0.50 d

Lever arm, $Z = d - \frac{a}{2} = 0.75d$

Ultimate moment of resistance, $M_u = (b \times 0.50d \times \frac{2}{3} f_{ck}) \times 0.75d = 0.25 f_{ck} b d^2$ for balanced section

Equating total compression = total tension

$b \times a \times \frac{2}{3} f_{ck} = A_{st} \times f_y$

$b \times 0.50d \times \frac{2}{3} f_{ck} = A_{st} \times f_y$

$A_{st} = \frac{fck\ b\ d}{3fy}$

For balanced section, $\frac{Ast \times fy}{bd \times fck} = \frac{1}{3}$

If in a beam, the ratio

I. If $\frac{Ast \times fy}{bd \times fck} < \frac{1}{3}$, the mode of failure is tension failure

II. If $\frac{Ast \times fy}{bd \times fck} > \frac{1}{3}$, the mode of failure is compression failure

III. If $\frac{Ast \times fy}{bd \times fck} = \frac{1}{3}$, the mode of failure is balanced failure

3.4 Shear strength of RC beams with FRP

The following presentation is based on ACI 318-95-1999

$V_n = V_c + V_s + V_{frp}$

Where, Vc= Shear capacity of concrete

V_s= Contribution of steel stirrups and bent up bars

V_{frp} = Contribution of FRP

V_n = Shear strength of a strengthened RC beam

$V_{frp} = \Phi_{frp} A_{frp} f_{frp} \frac{(sin\beta + cos\beta)}{Sfrp} d$

Where, f_{frp} = tensile strength of FRP

Φ_{frp} = 0.80,material reduction factor for the FRP

A_{frp} = Cross sectional area of a pair of FRP strips

β = angle of fiber orientation with respect to horizontal direction for the left side of the beam

d = effective depth of beam

s_{frp} = Spacing of FRP strips measured along the longitudinal axis

3.5 Flexural strength of RC beams with FRP

Existing research suggests that the ultimate flexural strength of FRP strengthened RC beams can be predicted using existing design approaches with modifications to account for the brittle nature of FRPs. The beam is deemed to have reached failure when either the concrete compressive strain attains the maximum usable strain 0.0035 according to BS 8110-1997 and/or the FRP reaches the rupture strain. The following presentation is based on British code BS 8110-1997.

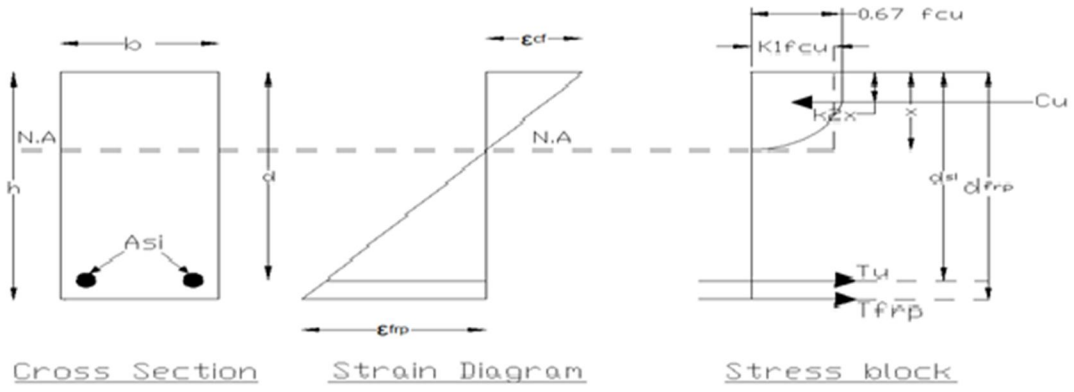

Fig. 3.3 Stress-strain diagram

The moment capacity of the beam M_u is determined by

$$M_u = k_1 \frac{f_{cu}}{\gamma_c} \; b\,x\left(\frac{h}{2} - k_2 x\right) + \sum_{i=1}^{n} \sigma_{si} A_{si}\left(\frac{h}{2} - d_{si}\right) + \sigma_{frp} A_{frp}\left(\frac{h}{2} - d_{frp}\right)$$

Where $K_1 = 0.67\left(1 - \frac{\epsilon co}{3\epsilon cf}\right)$ if $\epsilon_{co} \le \epsilon_{cf} \le 0.0035$

$$K_2 = \frac{\epsilon_{cf}/2 + \epsilon_{co}^2 / (12\,\epsilon_{cf}) - \epsilon_{co}/3}{\epsilon_{cf} - \epsilon_{co}/3} \quad \text{if } \epsilon_{co} \le \epsilon_{cf} \le 0.0035$$

The depth of neutral axis x can be determined by solving the following force equilibrium equation.

$$k_1 \frac{fcu}{\gamma c} \; \text{b x} + \sigma_{si} A_{si} + \sigma_{frp} A_{frp} = 0$$

Where x = neutral axis depth

d_{si} = the centroid of steel bars in layer i from the extreme concrete compression fiber

d_{frp} = the centroid of FRP from the extreme concrete compression fiber

h = the depth of the RC beam

ϵ_{cf} = strain at extreme compression fiber of concrete

ϵ_{frp} = strain in the FRP

ϵ_{si} = strain in the steel

ϵ_{co} = Compressive strain of unconfined concrete at peak stress = $\frac{1}{4100}\sqrt{\frac{fcu}{\gamma c}}$

ϵ_{u} = ultimate compressive strain of concrete

f_{cu} = cube compressive strength of concrete

b = beam width

K_1 = mean stress factor

σ_{si}= stress in steel bars

σ_{frp} = stress in FRP

A_{si} = total area of steel in layer i

n = total numbers of steel layers

A_{frp} = area of FRP

K_2 = centroid factor of the compressive force

F_{frp} = tensile strength of FRP

E_{frp} = modulus of elasticity of FRP

γ_{frp} = partial safety factor for FRP tensile strength

γ_s = partial safety factor for steel

γ_c = partial safety for concrete in flexure

3.6 Deflection of beams

The deflection of control beams are predicted for uniformly distributed loaded simply supported beams as per Annexure C of IS 456–2000. The deflection of FRP strengthened beams are predicted as per proposed model suggested by Gorji (2009).

Based on the transformed cracked section, the neutral axis depth Z can be solved from,

$\frac{1}{2} b Z^2 + (\alpha_s - 1) A_{sc} (Z - d_2) = \alpha_s A_{st} (d - Z) + \alpha_f A_f (h - z)$

Deflection

$$y = \frac{q\,[\ell^2 \varkappa\,(\ell-\varkappa) + \varkappa^2\,(\ell-\varkappa)^2]}{24 d_1^2\,[\,E_c A_c Z_1^2 + E_s A_{st} + E_s A_{sc} Z_2^2 + E_f A_f Z_3^2]}$$

Where E_c = modulus of elasticity of concrete

E_s = modulus of elasticity of steel

E_f = modulus of elasticity of FRP

A_{sc} = Area of compression steel

A_{st} = Area of tension steel

A_f = Area of FRP

Z = neutral axis depth

$Z_1 = \frac{\frac{2}{3}Z}{d-z}$ $Z_2 = \frac{Z - d_2}{d - Z}$ $Z_3 = \frac{h - Z}{d-z}$, $d_1 = d - z$

$\varkappa$ = distance from the support where deflection is required

q = load per unit length

ℓ = effective length of span

b = width of beam

h = depth of beam

d = effective depth, d_2 = effective cover to compression steel

$\alpha_s = E_s / E_c$, $\alpha_f = E_f / E_c$

CHAPTER 4

EXPERIMENTAL PROGRAMME

Experiments are conducted to study the flexural/shear capacity of RC rectangular beams with/without FRP using local available materials.

4.1 Geometry of beams

The geometry of all beams are 1300mm overall length, 1000mm effective length (bearing 150mm each side), 110mm width and 200mm depth with varying reinforcement as per design. The dimensions of all beams are kept same throughout the experiment. Provision of a 30mm diameter service hole is provided along longitudinal direction below the neutral axis in the tension zone of all beams for future strengthening using steel bars, FRP bars or strands in prestressed girders as per practical consideration. All the beams are initially designed as per limit state method of design, simply supported at both ends and applied with multiple concentrated loads equivalent to uniformly distributed load (UDL). All the beams in CB, RB, RF and RS series are gradually test loaded up to failure/collapse.

4.2 Materials

4.2.1 Cement

Portland Slag Cement (PSC) conforming to IS 455 of Konark Brand is used throughout the investigation. It is tested for its physical properties in accordance with Indian Standard specification. The specific gravity of cement was found as 3.10.

i. **Aggregates**

The coarse aggregate used in this investigation is crusher broken hard granite chips, maximum size is 20 mm with specific gravity 2.70, grading confirming to IS-383-1970.The fine aggregate used is clean river sand passing through 4.75 sieves with specific gravity of 2.50 and grading zone III confirming to IS-383-1970.

ii. Reinforcing Steel

All longitudinal reinforcement used is HYSD bars confirming to IS 1786: 1979. The stirrups used are 8 mm dia HYSD bars/6 mm dia mild steel bars. The tensile yield strength of HYSD bars used is obtained by testing in the Electronic UTM (FIE make) Model No.UTES 100.

iii. Fibers

Glass and Carbon fibers are used as reinforcing material for FRP. Epoxy is used as the binding material between fiber layers. Glass fibers manufactured by OWEN'S CORNING weighing 360 gms/sqm and Carbon fibers 8H SATIN (T-300) manufactured by TORAY Industries weighing 420 gms/sqm are used for this investigation. Before preparation of specimens test coupons are prepared for characterization of materials used for FRP strengthening. Glass fibers, carbon fibers and epoxy are used for manufacture of test specimens. The test coupons are prepared as per ASTM:D3039M-08 from the FRP plates.

4.2.5 Resin

Polymeric resins are used both as the matrix for the FRP and as the bonding adhesive between the FRP and the concrete. The latter function is of particular concern here, as weak adhesives can cause interfacial failures. Epoxy resins are generally used in the flexural and shear strengthening of beams. The success of the strengthening technique primarily depends on the performance of the epoxy resin used for bonding of FRP to concrete surface. Numerous types of epoxy resins with a wide range of mechanical properties are commercially available in the market. The epoxy resins are generally available in two parts, a resin and a hardener. The epoxy resin and hardener used in this study are Lapox L-12 and hardener K-6 respectively manufactured by Atual Limited System.

4.2.6 Water

Ordinary clean potable tap water free from suspended particles and chemical substances is used for mixing and curing of concrete throughout the experiment.

4.3 Form work

Fresh concrete being plastic requires good form work to mould it to the required shape and size. So the form work should be rigid and strong to hold the weight of wet concrete without bulging

anywhere. The form work used for concreting all specimens consists of two channels sections having adjustable nuts and bolts, slotted steel plates at the end to fix it to required size as per IS 14687 shown in Fig. 4.1. The joints at bottom and sides are sealed to avoid leakage of cement slurry. Mobil oil was then applied to the inner faces of form work. The bottom rests over thick polythene sheet laid over rigid AS floor. The reinforcement cage is then lowered, placed in position inside the form work carefully with a cover of 20mm on sides and bottom by placing concrete cover blocks. Sample of grill reinforcement used is shown in Fig. 4.2.

Fig.4.1 Typical Steel form

Fig.4.2 Sample of grill reinforcement

4.4 Concrete mix proportioning

The design of concrete mix is done as per guidelines of IS 10262: 2009 with a proportion of 1:1.85:3.70 by weight to achieve a grade of M25 concrete. The maximum size of coarse aggregate used is 20 mm. The water cement ratio is fixed at 0.50 and a slump of 50 to 55 mm.

4.5 Mixing of concrete

The mixing of concrete is done using a standard mechanical mixer complying with IS 1791 and IS 12119. First coarse and fine aggregates are fed alternately, followed by cement. Then required quantity of water is slowly added into the mixer to make the concrete workable until a uniform colour is obtained. The mixing is done for two minutes after all ingredients are fed inside the mixer as per IS 456-2000.

4.6 Compaction of concrete

All the specimens are compacted by using 30mm size needle vibrator for good compaction of concrete as per IS 2505. The sides of the form work are tamped with a hammer to get a neat finish. Good care is taken to avoid displacement of reinforcement cage inside the form work while vibrating the concrete. Finally, the top surface of concrete levelled, finished smooth by using a trowel and wooden float. After six hours, the specimen detail and date of concreting is written on top surface to identify it properly.

4.7 Curing of concrete

The specimens are taken out of the mould after 24 hours, shifted to concrete floor, covered all round with wet jute bags. Potable water is sprinkled 6 times per day to keep the jute bags wet, to allow concrete for perfect curing. The curing is continued for 28 days.

4.8 Strengthening of beams using FRP fabrics

During the process of strengthening, the FRP fabrics are bonded to the concrete surface using a suitable resin and hardner as per manufacturer’s instructions. The preparations of the concrete surface are a very important work. Following the available research papers as indicated, corners of concrete are rounded, uneven surface of concrete are evened using a grinder, followed by a iron filing and finally rough sand papering. The surface of concrete are grinded using rough

carborundum stones (used for cutting mosaic floors) followed by rough sand papering. The concrete surface is wiped using a linen wet cloth. This process is repeated three times to obtain even rough surface, corners rounded up and finally wiped using a clean piece of cloth. This procedure is followed to avoid premature debonding of FRP from concrete surface. Once the surface is prepared, FRP fabrics tailored to required size are kept ready for use. Epoxy resin is mixed with hardener as per manufacturer's instructions. In this case FRP fabric to be used is weighed, equal weight of epoxy resin is taken (50:50 by weight), kept in a plastic container, then 10% of hardener (with respect to the epoxy resin) by weight is taken, mixed with epoxy resin already in the plastic container, stirred by a stick until the mixture is in uniform colour.Then the epoxy resin is applied to the concrete surface with a hand brush uniformly, then one layer of composite fabric is placed over it, surface pressed-rolled with a iron hand roller to squeeze out excess of epoxy resin from the surface. Any air bubbles entrapped in the concrete-resin-fabric interface must be squeezed out and eliminated for perfect bonding. Then the second layer of epoxy resin is applied over the first layer of FRP already pressed over concrete surface, again second layer FRP fabric is placed over the first layer, pressed-rolled with a hand roller, excess resin squeezed out, any entrapped air bubble eliminated from the interface and finally pressed with hands over the concrete surface. The adhering process is repeated for the third time for some specimens in the experiment. In the process full contact between the epoxy resin, the layers of FRP fabrics and the concrete surface must be ensured to avoid premature debonding failure of FRP layers. This operation must be done very quickly to avoid hardening of epoxy resin-hardener mix and hand brush kept in the plastic container. The operation is carried out at room temperature, cured for minimum 3 days before testing.

4.9 Fabrication of GFRP/CFRP specimens for tensile strength

The following procedure and constituent materials are used for fabricating the plate and testing.

a) Carbon/glass woven roving as reinforcement
b) Epoxy as resin
c) Hardener as diamine (catalyst)
d) Polyvinyl alcohol as a releasing agent

Contact moulding in an open mould by hand lay-up is used to combine plies of woven roving with epoxy resin to form a laminate of required plies for testing as per the prescribed sequence. For this, a flat plywood rigid platform is selected. A thick plastic sheet is kept on the plywood platform, and a thin film of polyvinyl alcohol is applied on it as a releasing agent by use of spray gun. Lamination of fabrics started with the application of a gel coat (epoxy mixed with 10% hardener) deposited over the mould (plastic sheet) by hand brush, whose main purpose is to provide a smooth external surface and to protect the fabrics from direct exposure to environment. Fabric of 350×350 mm size of required numbers are cut from the roll of woven roving to form a laminate of required ply. Layers of fabric are placed on the mould one after the other applying a coat of epoxy by hand brushing on each layer. Each layer of fabric is pressed down using an iron roller, pressing and rolling continued until excess of epoxy, entrapped air if any are squeezed out to provide perfect bond between layers. This process is continued until required number of layers is achieved. Again, a plastic sheet is covered on the top of the laminate after applying polyvinyl alcohol on the sheet (face coming in the contact with the lamina) as releasing agent. Then, another flat plywood board is placed over it. Finally, a heavy flat metal rigid platform is kept over the plywood board for compressing purpose, cured for minimum 3 days, before transporting and cutting to exact size for testing of plates.

4.10 Experimental set up for testing of beams

All the specimens are tested in loading frame of the Structural Engineering Laboratory, National Institute of Technology, Rourkela. The testing procedures for all specimens are same. After curing for 28 days, control beams CB series are tested one by one applying load slowly up to failure load. Similarly, after curing for 28 days, CFRP/GFRP fabric in multiple layers, in variable lengths as per design are bonded to the concrete surface, cured for more than 3 days to RB, RF and RS series beams. The beams are tested one by one applying load slowly up to the failure load. In the testing arrangement, multiple concentrated loads equivalent to uniformly distributed load (UDL) is applied on all the beams gradually increased up to failure. The load is transmitted through two load cells, then to the spreader beams, finally to four steel blocks of 75mm width×125mm length placed over the test beam. Considering dispersion of load at 45^0 over the beam, the load is practically spread over the entire beam equivalent to UDL. The beam is placed over two steel roller bearings, kept over two steel pedestals at each end, leaving 150mm bearing

from either end with an effective span of 1000mm.The loading frame is capable of carrying the expected peak load without significant distortion .Loading is done by two hydraulic jacks of 500 KN capacity each. Three number of dial gauges are placed below the beam at quarter span, mid span and three-fourth span to measure deflection of the beam. The dial gauges are taken out, when these showed rapid deflection indicating imminent approach towards peak/failure load to avoid damage.

4.11 Loading pattern

The Fig.4.3 given below shows the typical test arrangement under multiple concentrated loads equivalent to uniformly distributed load done in the structural laboratory. The BM and SF diagrams are shown in Fig. 4.4.

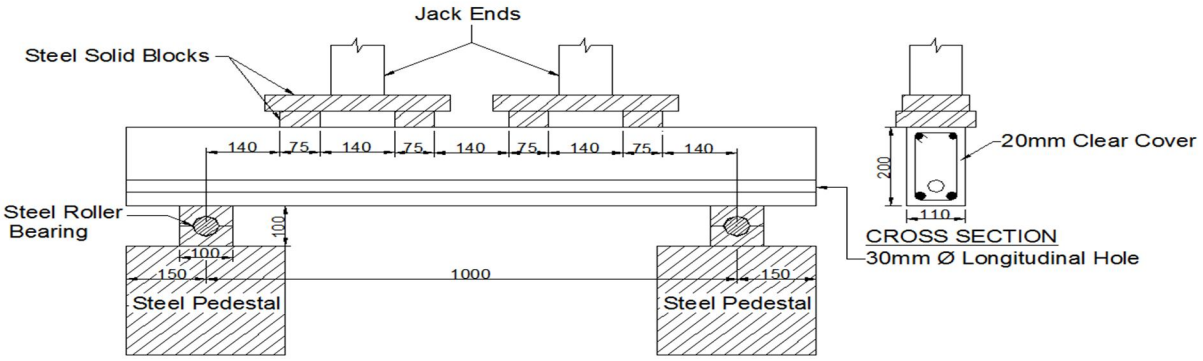

Fig. 4.3 Typical test arrangement under multiple concentrated loads

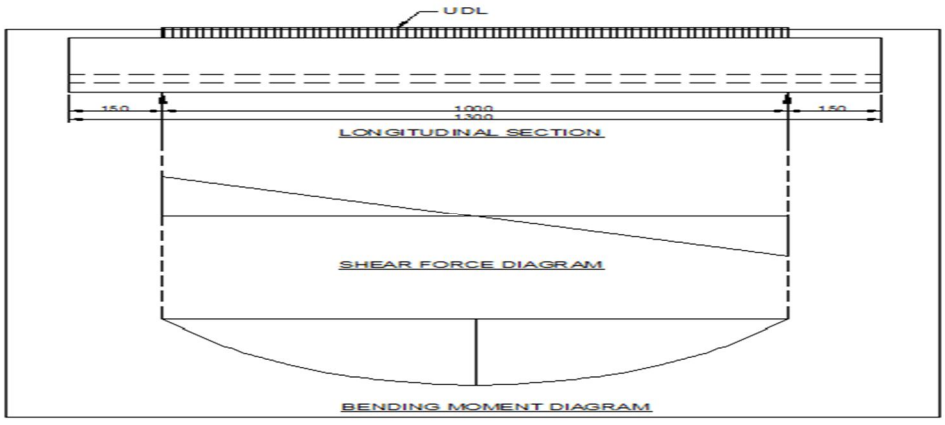

Fig. 4.4 Shear force and bending moment diagram

CHAPTER 5

RESULTS AND DISCUSSION

5.1 Introduction

This chapter describes the experimental results of CB series (control beams) , RF series (weak in flexure) and RS series (weak in shear) beams. Out of 15 beams, 4 are control beams without any FRP strengthening, one beam is made without any steel reinforcement, but strengthened with FRP, 5 beams are made weak in flexure, but strengthened in flexure with FRP and 5 beams are made weak in shear, but strengthened with shear with FRP fabrics in various configurations. All the 15 beams are tested up to failure. Prior to testing of beams, the tensile test results of reinforcing steel as per IS 1786-1985 and test results corresponding to tensile test of FRP laminates as per ASTM: D3039M-08 are presented. The compressive strength of controlled concrete cubes are also presented along with the flexural and shear strength of test beams. Their behavior throughout the test up to failure are described with respect to initial and ultimate load carrying capacity, deflection behaviour, rigidity, ductility, crack pattern and mode of failure.

5.2 Tensile strength of Reinforcing Steel

All the reinforcing steel used are of Shristhi brand and are tested to obtain tensile yield stress in an Electronic UTM Model No. UTES 100 shown in Fig. 5.1, stress-strain curve in Fig. 5.2 and the results in Table 5.1. The average yield strength used in the experiment fy =531 N/ mm^2.

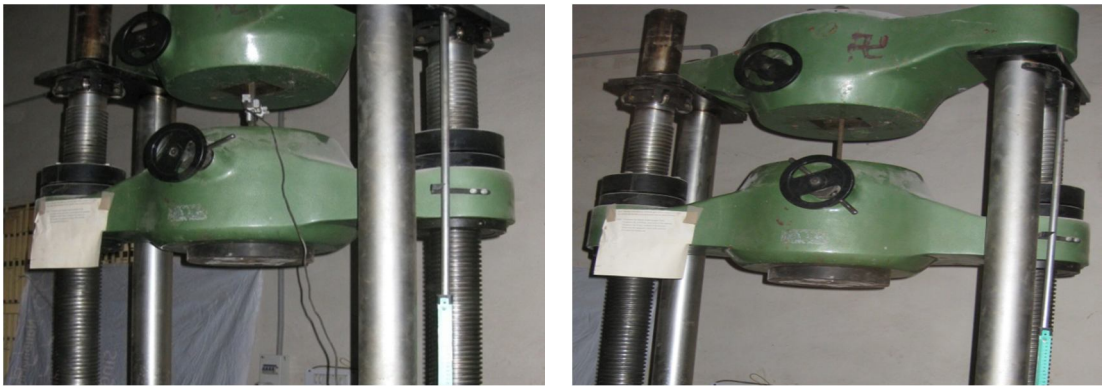

Fig.5.1 Tensile strength of steel in electronic UTM

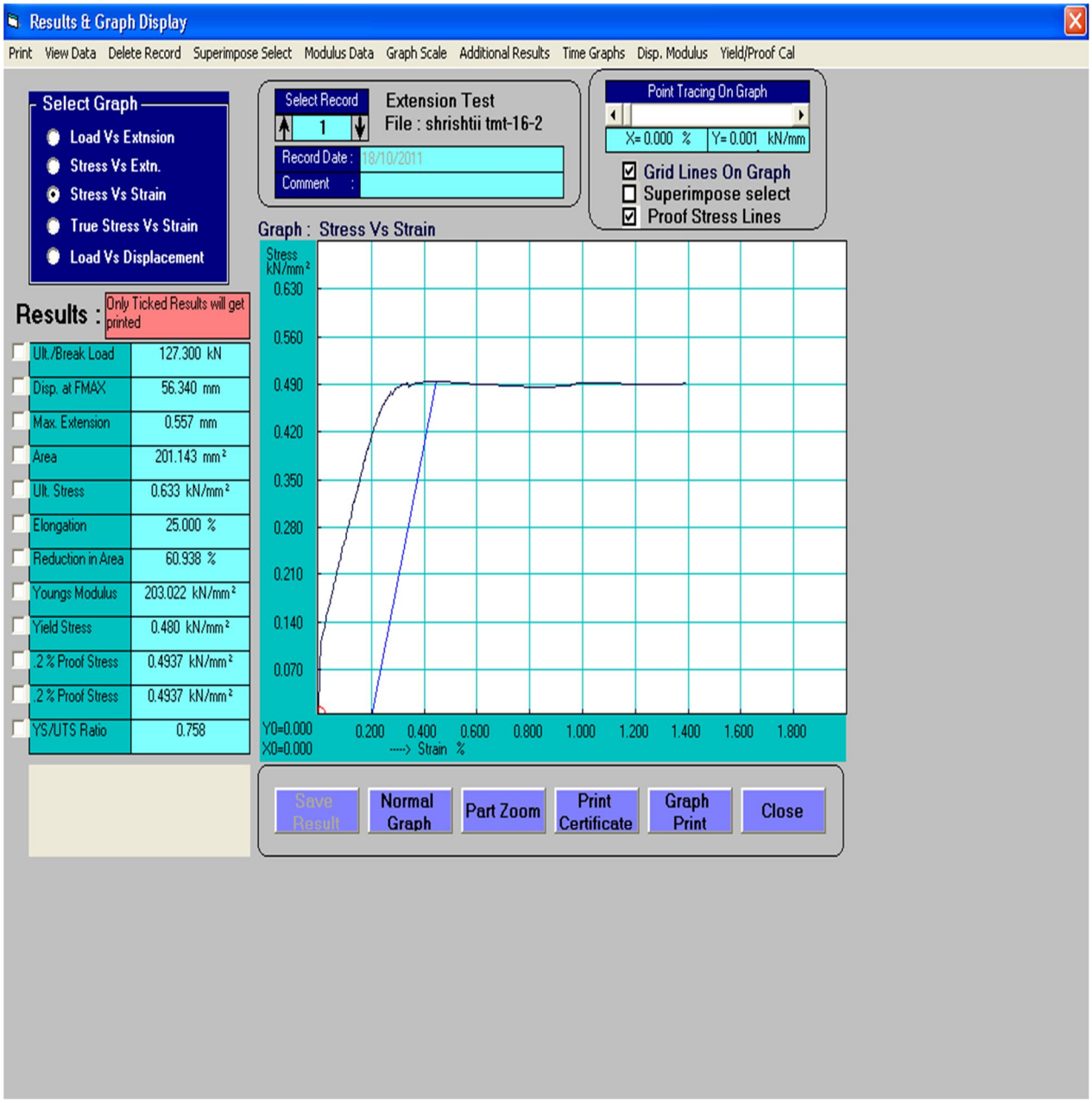

Fig. 5.2 Stress-strain curve for reinforcing steel

Table 5.1 Tensile test of reinforcing steel

Sl. no of sample	Diameter of bar tested (mm)	0.2% proof stress (yield strength) (N/mm^2)	Avg. Yield strength (N/mm^2)
1	16	506	494
2	16	495	
3	16	480	
4	12	595	578
5	12	560	
6	12	579	
7	10	530	529
8	10	535	
9	10	521	
10	8	520	523
11	8	527	
12	8	521	

5.3 Determination of Yield stress and Young's modulus of FRP

The yield stress (at 0.2% strain) and Young's Modulus are obtained experimentally by performing unidirectional tensile tests on specimens cut in longitudinal and transverse directions as prescribed in ASTM:D3039M-08 from the FRP plates fabricated earlier having constant rectangular size 250 mm length × 25mm width. The specimens are cut from the plates by a diamond cutter or by mechanically operated hex saw. After cutting, the sides are polished by sand paper. Three or more sample specimens are prepared from each plate of 2 PLY GFRP, 3 PLY GFRP and 2 PLY CFRP in this experiment, details shown in Table 5.2, 5.3 and 5.4 respectively. The specimens are tested in INSTRON 1195 universal testing machine. Each specimen is fixed in the upper jaw first, and gripped in the movable lower jaw having a gauge length of 150 mm. Gripping of specimen should as much as possible to prevent slippage. The load and extension are recorded digitally with the help of a load cell and an extensometer respectively. The specimen gradually loaded up to failure which is abrupt and sudden as the FRP

material is brittle in nature. The INSTRON 1195 machine shown in Fig. 5.3 directly indicated the yield stress, Young's Modulus, ultimate strength and plotted the load-deflection curve shown in Fig. 5.4.The test results of 2 PLY CFRP, 2PLY GFRP and 3 PLY GFRP fabrics are shown in Table 5.5, 5.6 and 5.7 respectively.

Table 5.2 Tensile strength of 2 layer Glass / epoxy laminates

Sample no.	Length of sample (mm)	Width of sample (mm)	Thickness of sample (mm)	Gauge length (mm)	Stress 0.2% Yield(MPa)	Young's Modulus (MPa)
1	250	26	1	150	255.4	20120
2	250	26	1	150	235.3	19470
3	250	26	1	150	232.4	17740
				Mean	241.0	19110

Table 5.3 Tensile strength of 3 layer Glass / epoxy laminates

Sample no.	Length of sample (mm)	Width of sample (mm)	Thickness of sample (mm)	Gauge length (mm)	Stress 0.2% Yield(MPa)	Young's Modulus (MPa)
1	250	24	1.3	150	240.9	19590
2	250	27	1.3	150	277.1	21890
3	250	26	1.3	150	201.7	18820
				Mean	239.9	20100

Table 5.4 Tensile strength of 2 layer Carbon / epoxy laminates

Sample no.	Length of sample (mm)	Width of sample (mm)	Thickness of sample (mm)	Gauge length (mm)	Stress 0.2% Yield(MPa)	Young's Modulus (MPa)
1	255	27.3	0.7	150	476.0	38540
2	255	28.2	0.7	150	571.1	39420
3	255	26.4	0.7	150	642.5	37350
				Mean	563.2	38440

Fig.5.3 Test of FRP plate in INSTRON 1195

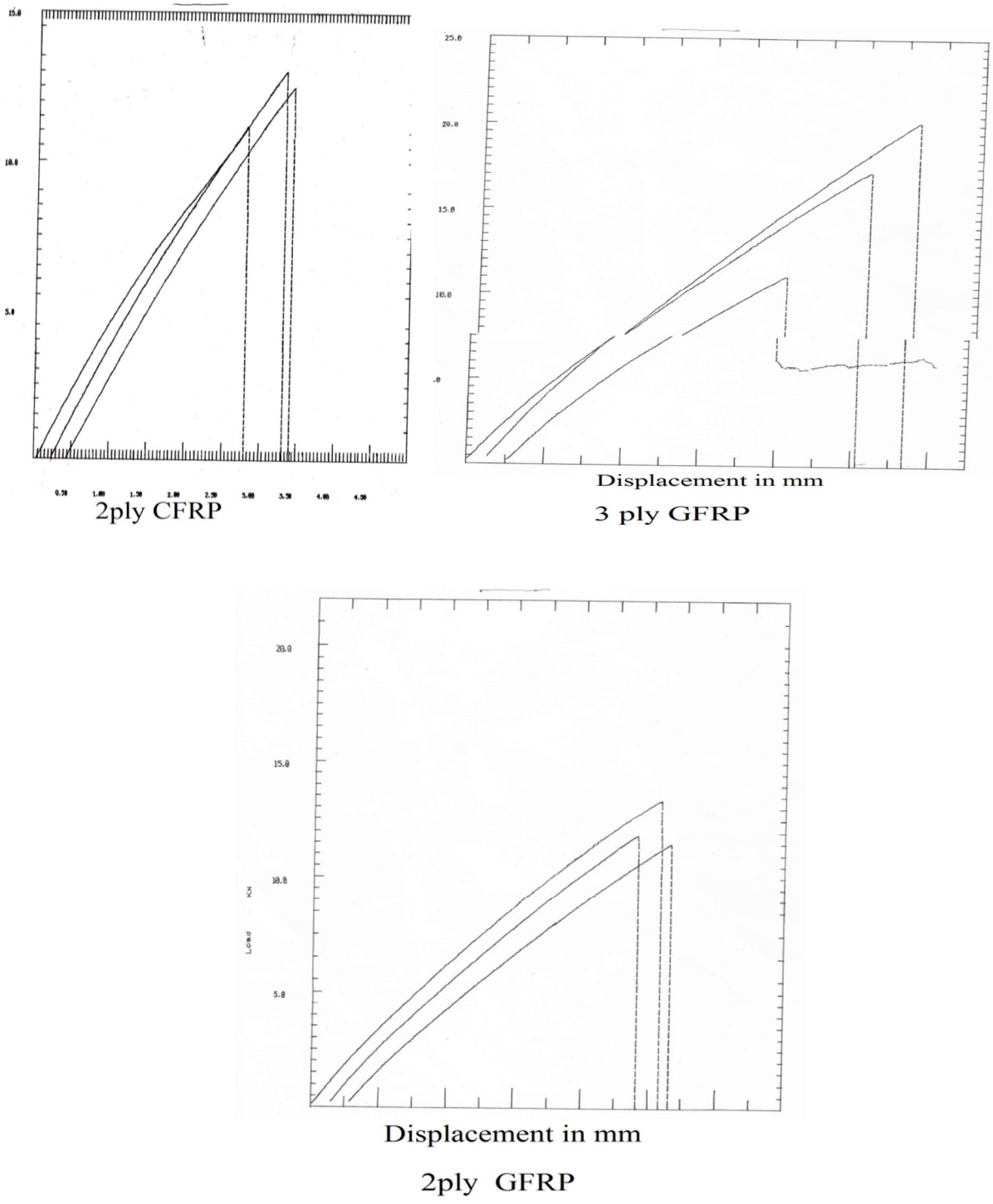

Fig.5.4 Stress-strain curve for FRP

DEPT.OF MET. & MAT. ENGG.

NIT, ROURKELA

Tensile Test of Metals: Instron Corporation

Series IX Automated Materials Testing System 1.26

Test Date: 19 July 2012, Sample type: ASTM

Sample Identification: 2 PLYCFRP

Interface Type: Data Systems Adapter

Machine Parameters of test:

Sample rate (pts/sec): 9.103 Humidity (%): 50

Crosshead speed (mm/min): 1.000 Temp (deg,F): 73

Full scale load range (KN): 100.0

Dimensions:	**Spec.1**	**Spec.2**	**Spec.3**
Width (mm)	27.0	27.0	27.0
Thickness (mm)	0.70	0.70	0.70
Spec.gauge len (mm)	150.0	150.0	150.0
Grip distance (mm)	100.0	100.0	100.0

Out of 3Specimens, 0 excluded

Table 5.5 Test Result 2 PLY CFRP

Spec. No.	Displment at Peak(mm)	Strain at Peak(%)	Load at Peak(KN)	Stress at Peak(MPa)	Displment at Break(mm)	Strain at Break(%)	Load at0.2% Yield(KN)	Stress at0.2% Yield(MPa)	Young's Modulus (Mpa)
1	2.767	1.845	11.14	589.7	2.767	1.845	8.996	476.0	38540
2	3.078	2.052	13.04	690.1	3.078	2.052	10.790	571.1	39420
3	2.981	1.987	12.49	661.0	2.981	1.987	12.140	642.5	37350
Mean.	2.942	1.961	12.23	646.9	2.942	1.961	10.640	563.2	38440
Stand. Devtin	0.159	0.106	0.98	51.7	0.159	0.106	1.580	83.6	1041

DEPT.OF MET. & MAT. ENGG

NIT, ROURKELA

Tensile Test of Metals: Instron Corporation

Series IX Automated Materials Testing System 1.26

Test Date: 19 July 2012, Sample type: ASTM

Sample Identification: 2 PLYGFRP

Interface Type: Data Systems Adapter

Machine Parameters of test:

Sample rate (pts/sec): 9.103 Humidity (%): 50

Crosshead speed (mm/min): 1.000 Temp (deg,F): 73

Full scale load range (KN): 100.0

Dimensions:	**Spec.1**	**Spec.2**	**Spec.3**
Width (mm)	26.0	26.0	26.0
Thickness (mm)	1.0	1.0	1.0
Spec. Gauge length (mm)	150.0	150.0	150.0
Grip distance (mm)	100.0	100.0	100.0

Out of 3Specimens, 0 excluded

Table 5.6 Test Result 2 PLY GFRP

Spec. No.	Displment at Peak(mm)	Strain at Peak(%)	Load at Peak(KN)	Stress at Peak(MPa)	Displment at Break(mm)	Strain at Break (%)	Load at0.2% Yield(KN)	Stress at0.2% Yield(MPa)	Young's Modulus (Mpa)
1	5.163	3.442	13.34	513.0	5.165	3.443	6.642	255.4	20120
2	4.599	3.066	11.89	457.3	4.599	3.066	6.117	235.3	19470
3	4.805	3.203	11.49	441.9	4.805	3.203	6.042	232.4	17740
Mean.	4.855	3.237	12.24	470.7	4.856	3.237	6.267	241.0	19110
Stand. Devtin	0.285	0.19	0.97	37.4	0.287	0.191	0.327	12.6	1231

DEPT.OF MET. & MAT. ENGG

NIT, ROURKELA

Tensile Test of Metals: Instron Corporation

Series IX Automated Materials Testing System 1.26

Test Date: 19 July 2012, Sample type: ASTM

Sample Identification: 3 PLY GFRP

Interface Type: Data Systems Adapter

Machine Parameters of test:

Sample rate (pts/sec): 9.103 Humidity (%): 50

Crosshead speed (mm/min): 1.000 Temp (deg,F): 73

Full scale load range (KN): 100.0

Dimensions:	**Spec.1**	**Spec.2**	**Spec.3**
Width (mm)	26.0	26.0	26.0
Thickness (mm)	1.3	1.3	1.3
Spec.gauge length (mm)	150.0	150.0	150.0
Grip distance (mm)	100.0	100.0	100.0

Out of 3Specimens, 0 excluded

Table 5.7 Test Result 3 PLY GFRP

Spec. No.	Displment at Peak(mm)	Strain at Peak(%)	Load at Peak(KN)	Stress at Peak(MPa)	Displment at Break(mm)	Strain at Break (%)	Load at0.2% Yield(KN)	Stress at0.2% Yield(MPa)	Young's Modulus (Mpa)
1	5.119	3.413	17.24	510.0	5.119	3.413	8.141	240.9	19590
2	5.494	3.663	20.13	595.7	5.494	3.663	9.365	277.1	21890
3	3.500	2.333	11.09	328.1	5.607	3.738	6.817	201.7	18820
Mean.	4.704	3.136	16.15	477.9	5.407	3.604	8.108	239.9	20100
Stand. Devtin	1.060	0.707	4.620	136.7	0.256	0.170	1.275	37.7	1597

5.4 Compressive Strength of Concrete Cubes

Six concrete cube specimens of 150 mm × 150 mm × 150 mm size taken during concreting of each CB, RF and RS series beams are tested on 7 days and 28 days shown in Fig. 5.5 and 5.6. The compressive strength obtained for CB, RF and RS series beams are presented in Table 5.8, Table 5.9 and Table 5.10 respectively.

Fig. 5.5 Testing of concrete cube

Fig. 5.6 Testing of concrete cube after failure

Table 5.8 Compressive strength of test cubes for CB series

Cube sample	Weight of cubes (Kg)	Cube strength after 7 days (N/mm^2)	7 days avg. Cube strength (N/mm^2)	Cube strength after 28 days (N/mm^2)	28 days avg. Cube strength (N/mm^2)
1	8.396	20.89	19.71	-	29.65
2	8.242	18.67		-	
3	8.300	19.56		-	
4	8.280	-		29.65	
5	8.342	-		31.39	
6	8.288	-		27.9	

Table 5.9 Compressive strength of test cubes for RF series

Cube sample	Weight of cubes (Kg)	Cube strength after 7 days (N/mm^2)	7 days avg. Cube strength (N/mm^2)	Cube strength after 28 days (N/mm^2)	28 days avg. Cube strength (N/mm^2)
1	8.235	20.49	20.46	-	30.33
2	8.278	20.36		-	
3	8.295	20.53		-	
4	8.204	-		29.87	
5	8.316	-		30.35	
6	8.268	-		30.78	

Table 5.10 Compressive strength of test cubes for RS series

Cube sample	Weight of cubes (Kg)	Cube strength after 7 days (N/mm^2)	7 days avg. Cube strength (N/mm^2)	Cube strength after 28 days (N/mm^2)	28 days avg. Cube strength (N/mm^2)
1	8.270	20.27	20.29	-	30.44
2	8.305	20.45		-	
3	8.295	20.14		-	
4	8.283	-		29.93	
5	8.295	-		30.39	
6	8.278	-		31.02	

5.5 Load prediction

The analysis of predicted load is made as per L.S.M (IS method) and U.L.M (Whitney's theory) for control beams, British code BS 8110-1997 for flexurally strengthened beams and ACI format ACI 318-95-1991 for shear strengthened beams. The predicted loads are calculated as follows.

5.5.1 Flexural capacity of beam by Limit State Method (IS456-2000)

Beam CB1 The cross section of the beam CB1 is shown in Fig.5.7

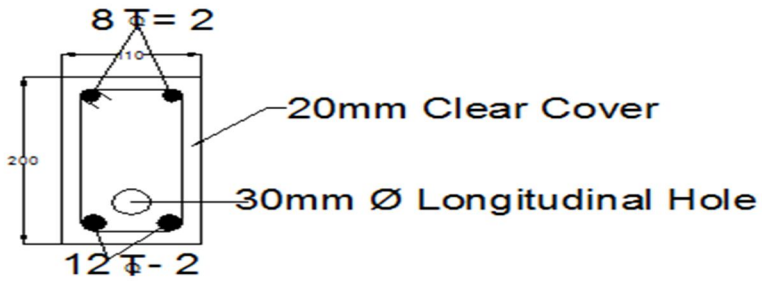

Fig. 5.7 Cross section CB1

Clear cover = 20mm, f_{ck} = 30 N/mm^2, f_y = 531 N/mm^2, A_{st}= 12Φ-2nos =226.28mm^2, d=174mm

It is a balanced section (slightly under reinforced), so MR is governed by steel area

$M_{lim} = 0.822 f_y A_{st} d$

$= 0.822 \times 531 \times 226.28 \times 174$

$= 17.19$ KNm

Bending Moment (BM) = $0.125 w \ell^2 = 17.19$ KNm

So load, w = 138 KN

Beam CB2 The cross section of the beam CB2 is shown in Fig.5.8

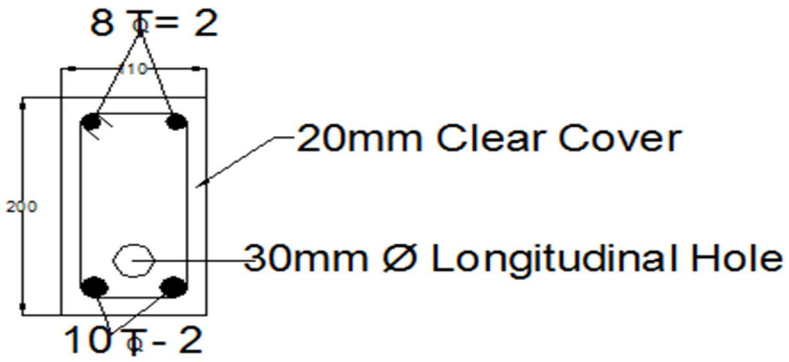

Fig.5.8 Cross section CB2

Under reinforced section, weak in flexure, but strong in shear.

Clear cover = 20mm, f_{ck} = 30 N/mm^2, f_y = 531 N/mm^2, A_{st}= 10Φ-2nos =157.14mm^2, d=175mm

It is a highly under reinforced section, so MR is governed by steel area.

$M_{lim} = 0.822 f_y A_{st} d$

$= 0.822 \times 531 \times 157.14 \times 175$

$= 12.0$ KNm

Bending Moment (BM) = $0.125w\ell^2$ = 12.0 KNm

So load, w = 96 KN

Beam CB3 The cross section of the beam CB3 is shown in Fig.5.9

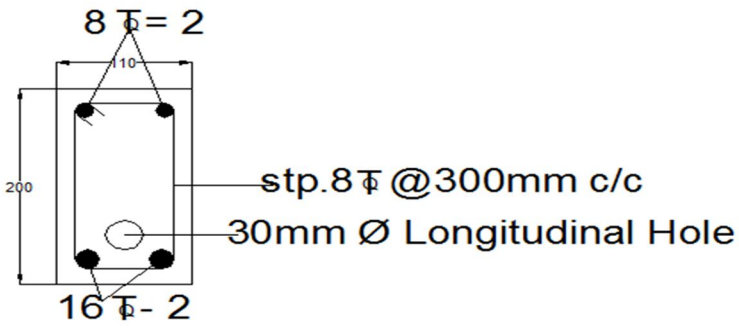

Fig. 5.9 Cross section CB3

Over reinforced section, weak in shear

Clear cover = 20mm, f_{ck} = 30 N/mm^2, f_y = 531 N/mm^2

A_{st}= 16Φ-2nos = 402.28mm^2, d = 172mm, b = 110mm, S_v = 8Φ @ 300 c/c

It is a highly over reinforced section, so MR is governed by shear only

$$\tau_c = \frac{Vu}{bd}$$

$V_u = V_{uc} + V_{us}$

$V_{uc} = \tau_{cmax} \times b\ d$

$\tau_{cmax} = 0.8\sqrt{f_{ck}} = 0.8\sqrt{30} = 4.382 N/mm^2$ as per BS 8110-1985

$V_{uc} = \tau_{cmax} \times b\ d = 4.382 \times 110 \times 172 = 82.91$ KN

$$V_{us} = \frac{fy\ Asv\ d}{Sv} = 531 \times 100.56 \times 172/300 = 30.62 \text{ KN}$$

V_u = 113.53 KN

So the initial cracking load = 2×113.53 = 227 KN

Beam CB4 The cross section of the beam CB4 is shown in Fig.5.10

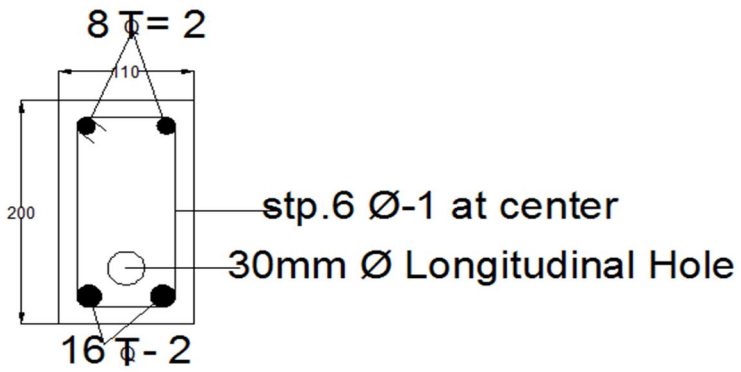

Fig. 5.10 Cross section CB4

Over reinforced section in flexure, very weak in shear. In fact no shear reinforcement is provided

Clear cover = 20mm, f_{ck} = 30 N/mm^2, f_y = 531 N/mm^2

A_{st}= 16Φ-2nos = 402.28mm^2, d = 172mm, b = 110mm

It is a highly over reinforced section, so MR is governed by shear only

$$\tau_c = \frac{Vu}{bd}$$

$V_u = V_{uc} + V_{us}$

$V_{uc} = \tau_{cmax} \times b\ d$

$\tau_{cmax} = 0.8\sqrt{f_{ck}} = 0.8\sqrt{30} = 4.382 N/mm^2$ [as per BS 8110-1985]

$V_{uc} = \tau_{cmax} \times b\ d = 4.382 \times 110 \times 172 = 82.91$ KN

$V_{us} = \frac{fy\ Asv\ d}{Sv} = 0$ since no shear reinforcement is provided

V_u = 82.91 KN

So the initial cracking load = 2×82.91 = 166 KN

5.5.2 Flexural capacity of beam by Ultimate Load Method (Whitney's Theory)

Beam CB1

Clear cover = 20mm, f_{ck} = 30 N/mm^2, f_y = 531 N/mm^2, A_{st}= 12Φ-2nos =226.28mm^2

d=174mm, b= 110mm

$$a = \frac{Ast\ fy}{2/3 fck\ b} = \frac{226.28 \times 531}{2/3 \times 30 \times 110} = 54.62\ mm^2 < d/2$$

So, the mode of failure is primary tension failure. Ultimate MR is governed by steel area.

$$M_u = T_u \times \text{Lever arm} = A_{st}\ f_y\ (d - \frac{a}{2}) = 17.63\ KNm$$

$W\ell^2/8 = 17.63$

Initial cracking load, w = 141 KN

Beam CB2

Clear cover = 20mm, f_{ck} = 30 N/mm^2, f_y = 531 N/mm^2, A_{st}= 10Φ-2nos =157.14mm^2

d=175mm, b= 110mm

$$a = \frac{Ast\ fy}{2/3 fck\ b} = \frac{157.14 \times 531}{2/3 \times 30 \times 110} = 37.93\ mm2 < d/2$$

So, the mode of failure is primary tension failure. Ultimate MR is governed by steel area

$$Mu = T_u \times \text{Lever arm} = A_{st}\ f_y\ (d - \frac{a}{2}) = 13.02\ KNm$$

$w\ell^2/8 = 13.02$

Initial cracking load , w = 104KN

Beam CB3

The beam is weak in shear.

Clear cover = 20mm, f_{ck} = 30 N/mm^2, f_y = 531 N/mm^2

A_{st}= 16Φ-2nos = 402.28mm^2, d = 172mm, b = 110mm, Stirrups S_v = 8Φ-2leg.stp.@ 300 c/c

It is a highly over reinforced section, MR is governed by shear only

$$\tau_c = \frac{Vu}{bd}$$

$V_u = V_{uc} + V_{us}$

$V_{uc} = \tau_{cmax} \times b\ d$

$\tau_{cmax} = 0.8\sqrt{f_{ck}} = 0.8\sqrt{30} = 4.382 N/mm^2$ as per BS 8110-1985

$V_{uc} = \tau_{cmax} \times b\ d = 4.382 \times 110 \times 172 = 82.91$ KN

$$V_{us} = \frac{fy\ Asv\ d}{Sv} = \frac{531 \times 100.56 \times 172}{300} = 30.62 \text{ KN}$$

V_u = 113.53 KN

So the initial cracking load = 2×113.53 = 227 KN

Beam CB4

Very weak in shear. In fact no shear reinforcement is provided

Clear cover = 20mm, f_{ck} = 30 N/mm^2, f_y = 531 N/mm^2

A_{st}= 16Φ-2nos = 402.28mm^2, d = 172mm, b = 110mm

MR is governed by shear only

$$\tau_c = \frac{Vu}{bd}$$

$V_u = V_{uc} + V_{us}$

$V_{uc} = \tau_{cmax} \times b\ d$

$\tau_{cmax} = 0.8\sqrt{f_{ck}} = = 0.8\sqrt{30} = 4.382 N/mm^2$ [as per BS 8110-1985]

$V_{uc} = \tau_{cmax} \times b\ d = 4.382 \times 110 \times 172 = 82.91$ KN

$V_{us} = \frac{fy\ Asv\ d}{Sv} = 0$ since no shear reinforcement is provided

V_u = 82.91 KN

So the initial cracking load = 2×82.91 = 166 KN

5.2.3 Shear strength of FRP strengthened beams (RS1 to RS5)

Beam RS1 The cross section of the beam RS1 is shown in Fig.5.11

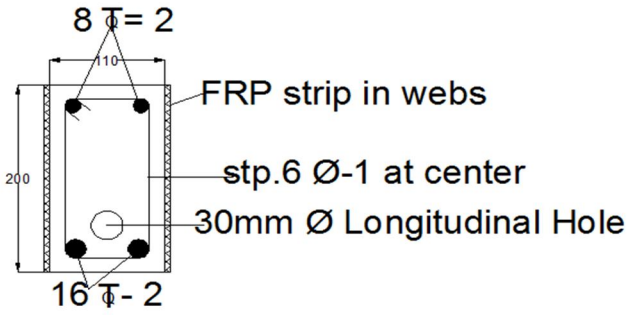

Fig. 5.11 Cross section RS1

Strengthened with 2 layers of GFRP in webs near supports for a length of 300mm

Vs = 0

$V_{frp} = \Phi_{frp}\ A_{frp}\ f_{frp}\ \frac{(sin\beta+cos\beta)}{Sfrp}\ d$

Φ_{frp} = 0.80, d = effective depth of beam = 164mm

$A_{frp} = t_{frp} \times w_{frp}$, t_{frp} = thickness of FRP = 1mm, w_{frp} = width of FRP = 300mm

f_{frp} = 241 N/mm^2, Angle β = (oriented 90^0 to the horizontal) = 90^0

$V_{frp} = \frac{0.80\times2\times300\times241}{300} \times 164$ =63.24 KN

V_n = 79+0+63.24=142.24

Initial cracking load=2×142.24=284.48, say 284 KN

Beam RS2 The cross section of the beam RS2 is shown in Fig.5.12

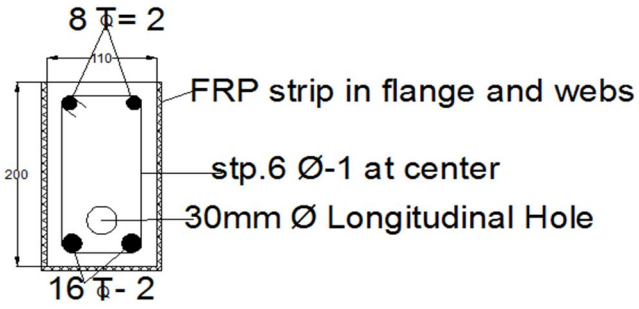

Fig. 5.12 Cross section RS2

Strengthened with two layers of GFRP U-jacketed in webs (in high shear zones) near each support for a length of 300mm.

Same as for RS1, Initial cracking load= 284 KN

Beam RS3 The cross section of the beam RS3 is shown in Fig.5.13

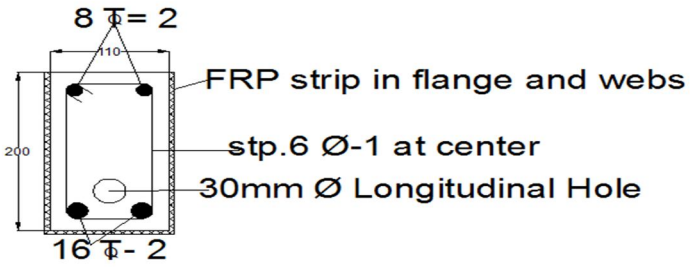

Fig. 5.13 Cross section RS3

Strengthened with three layers of GFRP U-jacketed in webs (in high shear zones) near each support for a length of 300mm.

$V_n = V_c + V_s + V_{frp}$

$V_c = \tau_{cmax} \times b\ d = 4.38 \times 110 \times 164 = 79015\ N = 79\ KN$

Vs = 0

$V_{frp} = \Phi_{frp} A_{frp} f_{frp} \frac{(sin\beta+cos\beta)}{Sfrp} d$

Φ_{frp} = 0.80, d = effective depth of beam = 164mm

$A_{frp} = t_{frp} \times w_{frp}$, t_{frp} = thickness of FRP = 1.3mm, w_{frp} = width of FRP = 300mm

= 2 sides × 1.3× 300 = 780 mm^2

$S_{frp} = w_{frp}$ = 300mm

f_{frp} = 239.9 N/mm^2, Angle β = (oriented 90^0 to the horizontal) = 90^0

$V_{frp} = \frac{0.80\times780\times239.9}{300} \times 164$ = 82.25 KN

V_n = 79+0+82.25=161.25 KN

Initial cracking load=2×161.25=322.50, say 323 KN

Beam RS4 The cross section of the beam RS4 is shown in Fig.5.14

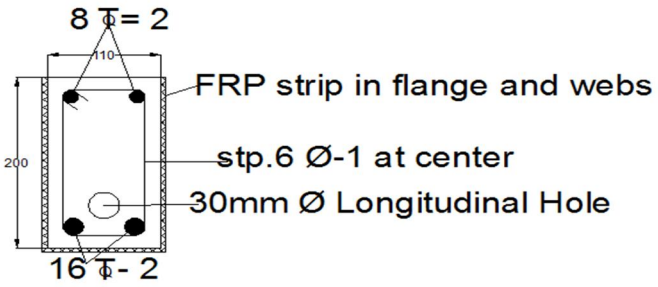

Fig. 5.14 Cross section RS4

Strengthened with two layers of GFRP 50mm wide inclined strips, 50mm gap in between strips on both sides of webs for the full length of span.

$V_n = V_c + V_s + V_{frp}$

$V_c = \tau_{cmax} \times b\ d = 4.38\times110\times164 = 79015$ N = 79 KN

Vs = 0

$V_{frp} = \Phi_{frp} A_{frp} f_{frp} \frac{(sin\beta+cos\beta)}{Sfrp} d$

Φ_{frp} = 0.80, d = effective depth of beam = 164mm

$A_{frp} = t_{frp} \times w_{frp}$, t_{frp} = thickness of FRP = 1mm, w_{frp} = width of FRP = 50mm,two sides of web

f_{frp} = 241 N/mm^2, Angle β = (oriented 90^0 to the horizontal) = 90^0

$V_{frp} = \frac{0.80\times2\times50\times241}{50} \times 164 = 63.24$ KN

$V_n = 79+0+63.24=142.24$ KN

Initial cracking load=2×142.24=284.48, say 285 KN

Beam RS5 The cross section of the beam RS5 is shown in Fig.5.15

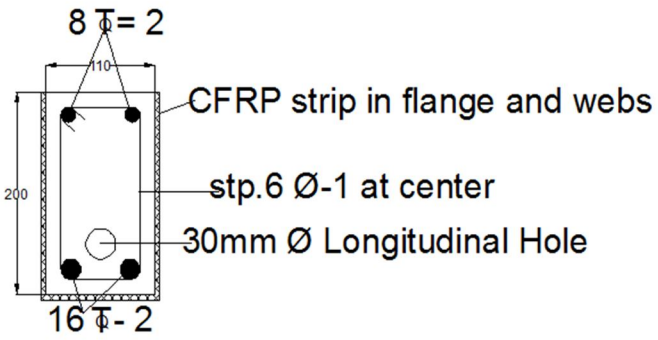

Fig. 5.15 Cross section RS5

Strengthened with two layers of GFRP U-jacketed in webs (in high shear zones) near each support for a length of 300mm.

$V_n = V_c + V_s + V_{frp}$

$V_c = \tau_{cmax} \times b\ d = 4.38\times110\times164 = 79015$ N = 79 KN

Vs = 0

$V_{frp} = \Phi_{frp} A_{frp} f_{frp} \frac{(sin\beta+cos\beta)}{Sfrp} d$

$\Phi_{frp} = 0.80$, d = effective depth of beam = 164mm

$A_{frp} = t_{frp} \times w_{frp}$, t_{frp} = thickness of FRP = 0.70 mm, w_{frp} = width of FRP = 300mm

= 2 sides × 0.70 × 300 = 420 mm^2

$S_{frp} = w_{frp}$ = 300mm

f_{frp} = 563.2 N/mm^2, Angle β = (oriented 90^0 to the horizontal) = 90^0

$V_{frp} = \frac{0.80 \times 420 \times 563.2}{300} \times 164$ = 103.45 KN

V_n = 79+0+103.45=182.45 KN

Initial cracking load=2×182.45=364.9, say 365 KN

5.5.4 Flexural strength of FRP strengthened beams (RF1 to RF5) (BS 8110- 1997)

Beam RF1 The cross section of the beam RF1 is shown in Fig.5.16

The factor of safety γ_{frp}, γ_s, γ_c are taken as unity as ultimate load of the FRP strengthened beam is required here.

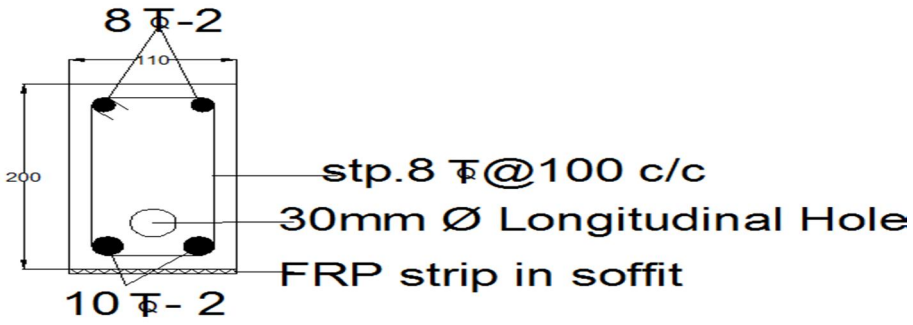

Fig. 5.16 Cross section RF1

The depth of neutral axis x can be determined by solving the following force equilibrium equation.

$$k_1 \frac{fcu}{\gamma c} \; b\, x + \sigma_{si}\, A_{si} + \sigma_{frp}\, A_{frp} = 0$$

f_{cu} = 30N /mm^2, $\gamma_c = 1$,

$$\epsilon_{cf} = \frac{1}{4100} \sqrt{\frac{fcu}{\gamma c}} = \frac{1}{4100} \sqrt{\frac{30}{1}} = 1.336 \times 10^{-3}$$

Assuming crushing of concrete, limiting value of $\epsilon_{cf} = 0.0035$

$$K_1 = 0.67 \left(1 - \frac{\epsilon co}{3 \epsilon cf}\right) = 0.585$$

$$K_2 = \frac{\epsilon_{cf}/2 + \epsilon_{co}^2 \,/\, (12\, \epsilon_{cf}) - \epsilon_{co}/3}{\epsilon_{cf} - \epsilon_{co}/3} = 0.441$$

σ_{si} = 531 N/mm^2, A_{si} = 2-10Φ = 157.14mm^2, $A_{frp} = t_{frp} \times b_{frp}$ = 100mm^2

Mean value of σ_{frp} from testing = 241 N/mm^2, d_{si} = 175mm

Putting all above values in the equation given below

$$k_1 \frac{fcu}{\gamma c} \; b\, x + \sum_{i=1}^{n} \sigma_{si}\, A_{si} + \sigma_{frp}\, A_{frp} = 0$$

x = -56.96mm

Moment of resistance

$$M_u = k_1 \frac{fcu}{\gamma c} \; b\, x \left(\frac{h}{2} - k_2 x\right) + \sum_{i=1}^{n} \sigma_{si}\, A_{si} \left(\frac{h}{2} - d_{si}\right) + \sigma_{frp}\, A_{frp} \left(\frac{h}{2} - d_{frp}\right)$$

Substituting all the values in the above equation, M_u = -22.667 KNm

Moment of resistance $w\ell^2/8$ = 22.667, neglecting – sign

Initial cracking load w = 181 KN as factor of safety is taken as unity for all material strength.

The above derivative also applies to **RF2 / RF4 / RF5**,

Where MR = 22.667 and cracking load w = 181 KN

Beam RF3 The cross section of the beam RF3 is shown in Fig.5.17

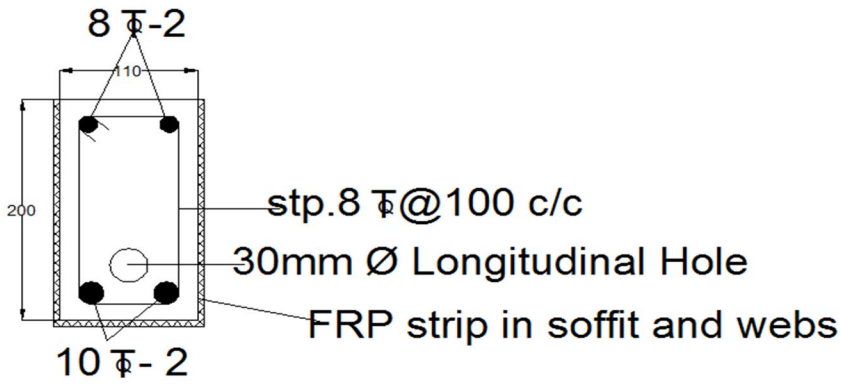

Fig. 5.17 Cross section RF3

The depth of neutral axis x can be determined by solving the following force equilibrium equation.

$$k_1 \frac{fcu}{\gamma c}\ b\ x + \sum_{i=1}^{n} \sigma_{si}\ A_{si} + \sigma_{frp}\ A_{frp} = 0$$

As per above

$K_1 = 0.585$, $f_{ck} = 30\ N/mm^2$, $\gamma_c = 1$, b= 110mm, $\sigma_{si} = 531\ N/mm^2$, $K_2 = 0.441$

$A_{si} = 2\text{-}10\Phi = 157.14mm^2$, $A_{frp} = t_{frp} \times b_{frp} = 1.3 \times 110mm^2 = 143mm^2$

Mean value of σ_{frp} from testing = $239.9\ N/mm^2$, $d_{si} = 175mm$

Putting these values in the above equation

x = -61mm

Moment of resistance

$$M_u = k_1 \frac{fcu}{\gamma c}\ b\ x\ (\frac{h}{2} - k_2 x) + \sigma_{si}\ A_{si}\ (\frac{h}{2} - d_{si}) + \sigma_{frp}\ A_{frp}\ (\frac{h}{2} - d_{frp})$$

Substituting all the appropriates values in the above equation, M_u = -24.633 KNm

Moment of resistance $w\ell^2/8 = 24.633$, neglecting –ve sign

Initial cracking load w = 197 KN as factor of safety is taken as unity for all material strength.

Beam RB1

No reinforcement is provided.1000mm length 2 layers of GFRP U-wrapped for the full span.

$$k_1 \frac{fcu}{\gamma c} \; b\, x + \sigma_{si}\, A_{si} + \sigma_{frp}\, A_{frp} = 0$$

As before f_{cu} = 30 N/mm^2, γ_c = 1, K_1 = 0.585, A_{si} = 0, σ_{si} =531 N/mm^2, K_2 = 0.441

Mean value of σ_{frp} from testing = 241 N/mm^2, $A_{frp} = t_{frp} \times b_{frp}$ = 110mm^2

Substituting all the appropriates values in the above equation, x = -13.732mm

Moment of resistance

$$M_u = k_1 \frac{fcu}{\gamma c} \; b\, x \left(\frac{h}{2} - k_2 x\right) + \sum_{i=1}^{n} \sigma_{si}\, A_{si} \left(\frac{h}{2} - d_{si}\right) + \sigma_{frp}\, A_{frp} \left(\frac{h}{2} - d_{frp}\right)$$

Substituting all the appropriates values in the above equation, M_u = -5.462 KNm

Moment of resistance, $w\ell^2/8$ = 5.462, neglecting –ve sign

Initial cracking load w = 44 KN, factor of safety is taken as unity for all material strength

5.6 Testing of beams, crack pattern and failure mode

All the 15 beams are tested one by one in the loading frame. Three dial gauges are fixed below the beam each one at quarter span, mid span and three-fourth span. The load is gradually increased up to failure. The deflections are recorded up to initial cracking load. After the needles in the dial gauge rotated rapidly indicating approach of imminent failure, the dial gauges are removed to save from damage during failure of beams.

Beam CB1

The geometry and reinforcement in the beam is shown in Fig.5.18. The beam is provided with balanced (slightly under reinforced) reinforcement. It is gradually loaded up to failure. The loading of beam, crack pattern with failure mode and load-deflection curve is shown in Fig. 5.19,

5.20 and 5.21 respectively given below. Hair cracks are appeared at mid span bottom, progressed upwards, gradually cracks widened, yielding of steel seen, then crushing of concrete at mid span top and failure occurred. It is a pure flexural failure. The theoretical cracking load as per LSM and ULM of design is 138 KN and 141 KN respectively. The experimental results showed an initial cracking load of 210 KN and ultimate load of 292KN shown in Table 5. 11.

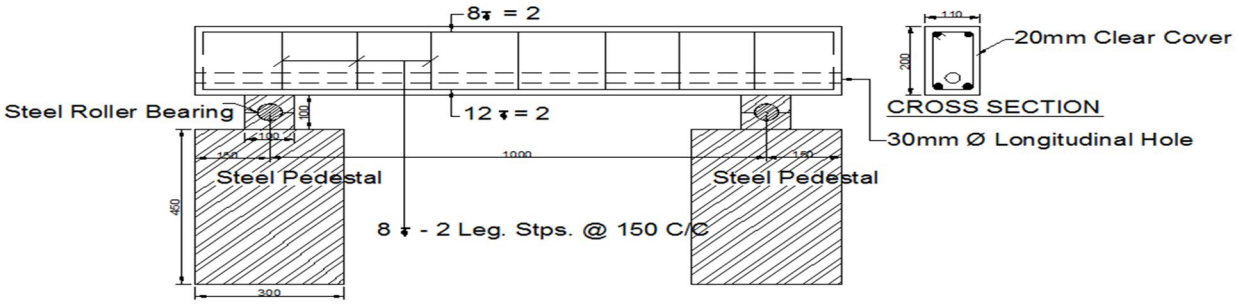

Fig. 5.18 Longitudinal section beam CB1

Fig 5.19 Loading arrangement beam CB1

Fig. 5.20 Failure of beam CB1

Table 5.11 EXPERIMENTAL RESULT OF CONTROL BEAMS

Beam specimen	Type of beam	Reinforcement provided – Tor steel			Initial Cracking/ Ultimate Load (KN)				Deflection (mm)			Deflection Load KN
		Top	Bottom	Shear	Limit state method	Ultimate load method	Experimental result		1/4 span	Mid span	3/4 span	
							Cracking load	Ultimate load				
CB1	Balanced	8 ϕ - 2	12 ϕ - 2	8 ϕ @ 150 C/C	138	141	210	292	0.97	1.15	1.00	110
CB2	Weak in flexure but strong in shear	8 ϕ - 2	10 ϕ -2	8 ϕ @ 100 C/C	96	104	120	170	1.35	2.48	1.35	110
CB3	Weak in shear but strong in flexure	8 ϕ - 2	16 ϕ -2	8 ϕ @ 300 C/C	227	227	290	367	3.1	3.35	2.82	340
CB4	Weak in shear but strong in flexure	8 ϕ - 2	16 ϕ -2	6 ϕ – 5 nos	166	166	160	360	2.36	2.45	2.15	260

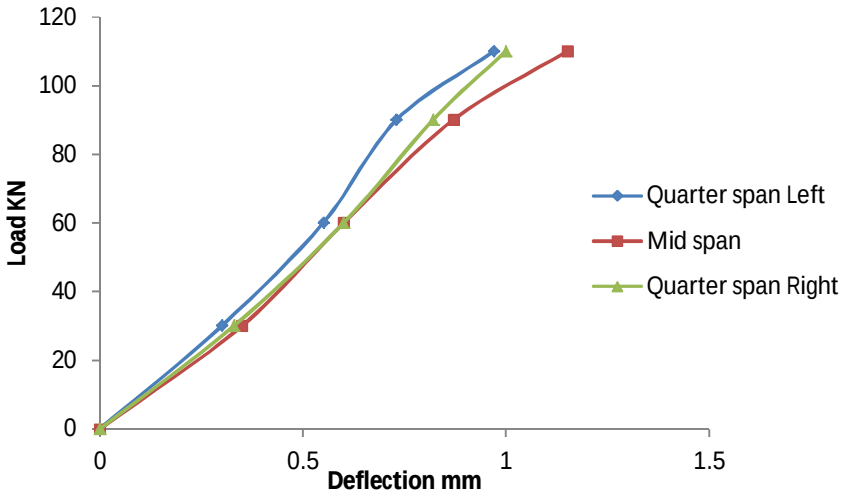

Fig.5.21 Load-deflection curve beam CB1

Control beam CB2

The geometry and reinforcement in the beam is shown in fig.5.22. The reinforcement is provided so as to make the beam weak in flexure but strong in shear. The beam is made weak in flexure, but strong in shear by providing suitable reinforcement. It is gradually loaded up to failure. The crack pattern, mode of failure and load-deflection curve is shown in the Fig. 5.23, 5.24 and 5.25 respectively. Small hair cracks appeared at mid span bottom, progressed upwards, crack widened, yielding of tensile steel were seen, followed by crushing of concrete at mid span top. It is purely a flexural failure. The theoretical cracking load as per LSM and ULM of design was 96 KN and 104 KN respectively. The experimental results showed an initial cracking load 120 KN and ultimate load of 170KN as shown in the Table 5.11.

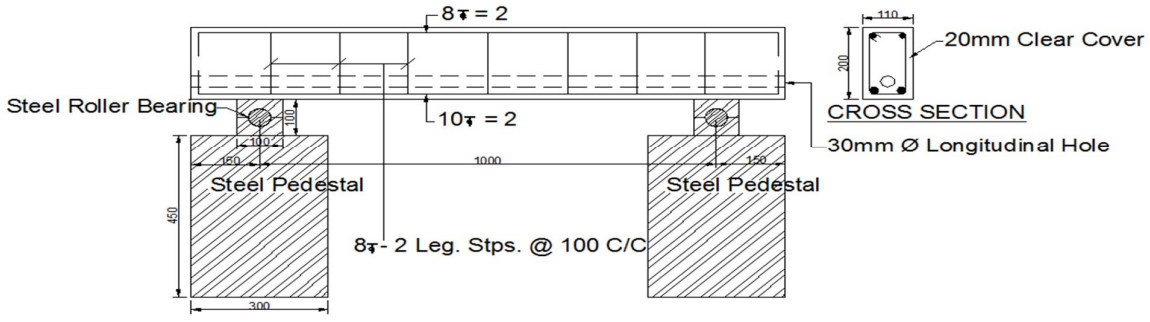

Fig. 5.22 Longitudinal section beam CB2

Fig.5.23 Crack pattern beam CB2

Fig.5.24 Failure of beam CB2

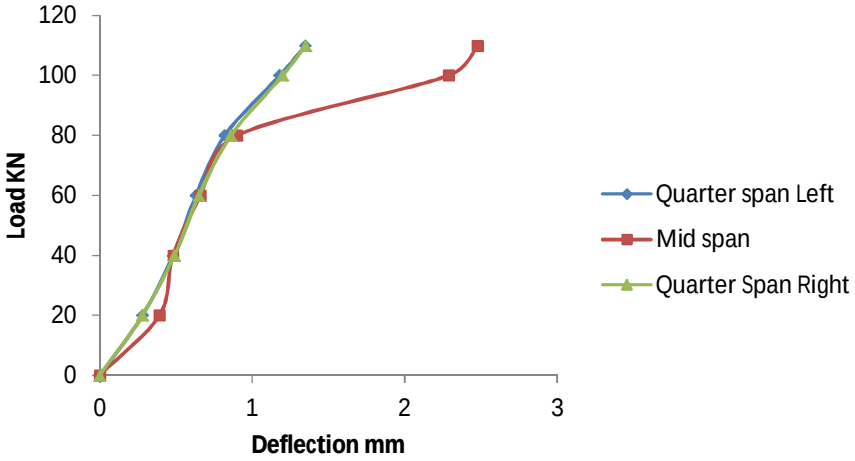

Fig.5.25 Load-deflection curve beam CB2

Control beam CB3

The geometry and reinforcement in the control beam CB3 is shown in fig.5.26. The reinforcement is provided so as to make the beam weak in shear but strong in flexure. It is gradually loaded up to failure. The mode of failure and load-deflection curve is shown in the Fig. 5.27 and 5.28 respectively. Inclined hair cracks appeared near one support from bottom, then crack appeared in the other support, cracks progressed upwards and widened gradually, went up to top of beam followed by crushing of concrete along the crack line and top, where the shear crack meets the beam top. It is a pure shear failure. The theoretical cracking load as per LSM of design is 227 KN. The experimental results showed an initial cracking load of 290 KN and ultimate load of 367 KN shown in the Table 5. 11.

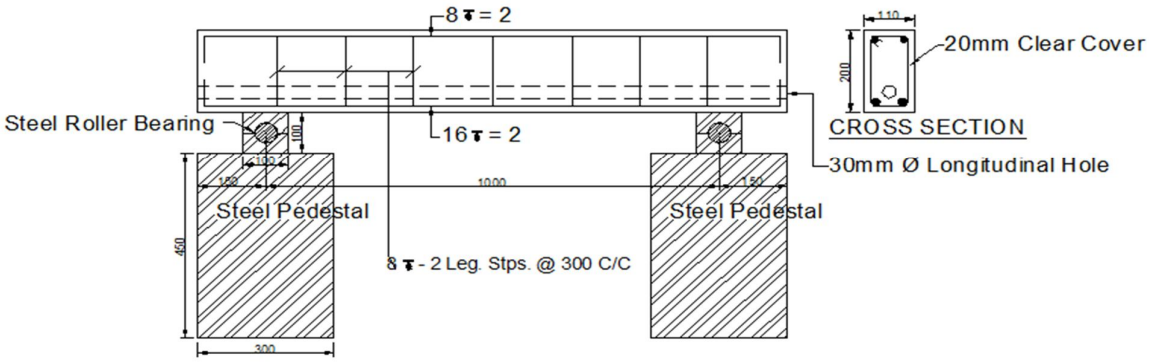

Fig.5.26 Longitudinal section beam CB3

Fig.5.27 Failure of beam CB3